Variability of light absorption coefficients by different size fractions of suspensions in the southern Baltic Sea

Justyna Meler[1], Dagmara Litwicka[1], Monika Zabłocka[1]

[1]Institute of Oceanology Polish Academy of Sciences, Powstańców Warszawy 55, 81-712 Sopot, Poland

5   *Correspondence to*: Justyna Meler (jmeler@iopan.pl)

Abstract. Measurements of light absorption coefficients by particles suspended in seawater ($a_p(\lambda)$), by phytoplankton ($a_{ph}(\lambda)$) and detritus ($a_d(\lambda)$) were carried out in the Baltic Sea waters. Measurements were performed for the original (unfiltered) seawater samples and the four selected size fractions: pico-particles with diameters (0.2-2 μm), ultra-particles with diameters (2-5 μm), nano-particles with diameters (5-20 μm) and micro-particles (20-200 μm). Chlorophyll *a* (Chl*a*) concentrations and

10   total suspended particulate matter (SPM) concentrations were determined. The proportions of particles from the size classes (micro, nano, ultra and pico) in the total light absorption by particles, phytoplankton and detritus were determined. Particles with sizes < 5 μm (i.e. pico and ultra-particles) had the largest contribution to the total particles absorption - an average of 38% and 31%. Particles of 5-20 μm accounted for approximately 20% of all particles and phytoplankton and 29% of the detritus. The contribution of large particles > 20 μm averaged 5-10%.

15   The average chlorophyll-specific and mass-specific light absorption coefficients, i.e. light absorption coefficients normalized to Chl*a* and to SPM concentration, were determined for all size fractions. The determined average chlorophyll-specific light absorption coefficients $a_p^{(Chl a)}(\lambda)$, $a_d^{(Chl a)}(\lambda)$ and $a_{ph}^{(Chl a)}(\lambda)$, along with standard deviations, do not allow clear separation of the individual fractions. For mass-specific light absorption coefficients, $a_p^{(SPM)}(\lambda)$, $a_d^{(SPM)}(\lambda)$ and $a_{ph}^{(SPM)}(\lambda)$, it is possible to distinguish between large particle fractions (microplankton – 20-200 μm) and small and medium particle fractions

20   (0.2-20μm).

1 Introduction

The biogeochemical and optical properties of coastal waters vary greatly due to high biological productivity, input of terrestrial material and resuspension of benthic matter (D'Sa, Miller and Del Castillo, 2006; Hoepffner and Sathyendranath, 1992). Additionally, these regions are particularly sensitive to environmental changes. This is due to changes in the populations of

25   phytoplankton and other particles in these ecosystems. Hence, their hydrographic and biogeochemical conditions can change in a short time. Knowledge of the size structure of phytoplankton populations and the effect of mineral and detritus particle sizes on light absorption is essential to better determine the impact of climate change on coastal marine systems (e.g., Le Quéré et al., 2005).

Seawater suspended particle matter (SPM) is an unknown mixture of organic and inorganic compounds, and its
30   composition varies spatially and temporally as a function of various physical (e.g., tides) and biogeochemical (e.g.,
phytoplankton blooms) factors (D'Sa and Ko, 2008; Eleveld et al., 2014). The variability of the type and source of particles
present in the marine environment implies the variability of its absorption properties in time and space. Accurate linking of
inherent optical properties (IOP) with measurements and predictions of particle population characteristics remains a major
scientific challenge, especially in optically complex waters. (McKee and Cunningham, 2006; Davies et al., 2014), which also
35   includes the Baltic Sea. The absorption properties of particles suspended in the water column vary significantly depending on
their type. The light absorption coefficient by suspended phytoplankton organisms, $a_{ph}(\lambda)$, is related to the composition of
pigments contained in algal cells and its spectral shape has two characteristic maxima (approximately 400-490 nm and 660-
690 nm). For the remaining suspended particles (detritus and mineral particles), the light absorption spectrum, $a_d(\lambda)$, is
characterized by a monotonic decline of exponential shape. The relationships between the coefficients $a_{ph}(\lambda)$ and $a_d(\lambda)$ and the
40   concentration of suspended substances present in the water has been the subject of research of many authors (Babin et al.,
2003; Woźniak et al., 2011, 2022; Meler et al., 2016 a,b, 2017, 2018; Castagna et al., 2022). The common knowledge is that
changes in the spectral shapes of the absorption coefficients follow the changes in size distribution of particles. For
phytoplankton, in particular, it has been shown that small phytoplankton exhibit higher absorption coefficients for short blue
wavelengths and more pronounced maxima compared to large phytoplankton cells. The larger the phytoplankton cells, the
45   greater the 'flattening' of the absorption spectrum (Morel and Bricaud, 1981; Sathyendranath et al., 1987; Ciotti et al., 2002).

Chlorophyll a (Chl$a$) concentration is a measure of phytoplankton biomass and, together with the size structure of
phytoplankton populations, are key ecological indicators in the marine environment (Platt and Sathyendranath, 2008). Changes
in these indicators can help detect how the marine ecosystem may respond to natural variability (e.g., innate climate variations)
and antropogenic changes (e.g., anthropogenic climate change). The light absorption properties depend on the physical and
50   chemical nature of the water and its constituents and therefore can provide biogeochemically useful information about the
composition of the particulate matter suspended in water.

The characteristics of the spectral coefficient $a_{ph}(\lambda)$ can be used to infer the size of phytoplankton, as well as
taxonomic information. These techniques are not as sensitive as direct pigment analyzes, especially in optically complex waters
with high spatial and temporal variability both in terms of phytoplankton and detritus concentration and composition (Bricaud
55   and Stramski, 1990; Bricaud et al., 2004; Ciotti et al., 2002; Mouw et al., 2017). However, direct measurements of the light
absorption coefficient of suspended particles can provide useful information on the size of phytoplankton, which can be used
as a basis for methods for estimating the size structure of phytoplankton populations (Bidigare et al., 1989; Moisan et al., 2011;
Organelli et al., 2013; Zhang et al., 2015).

The variability of light absorption coefficients by different size fractions of phytoplankton in the natural environment
60   has so far been described only by Ciotti et al. (2002) for the Bering Sea and the Oregon coast. Ciotti et al. (2002) found that
more than 80% of a_{ph} variability can be explained by the combined effects of dominant size class and pigment variability and
developed a two-component model that relates seawater samples to phytoplankton size structure. The shape of the

phytoplankton light absorption spectra can be reproduced by the size parameter (Sf). Sf describes the contribution of two basis vectors representing the extreme cases of the light absorption spectra shapes (that is, the light absorption spectra normalized

65 to their spectral mean in the 400-700 nm range) corresponding to 100% dominance picoplankton and 100% microplankton in the phytoplankton population (Ferreira et al., 2013). The total light absorption in seawater can be obtained from satellite data using the models of Loisel and Stramski (2000) and Loisel and Poteau (2006) by taking the absorption coefficients by phytoplankton and detritus together with dissolved organic matter obtained from analytical decomposition or nonlinear optimization (Ciotti et al., Bricaud, 2006; Bricaud et al., 2012). Further models of absorption depending on size fractions were

70 proposed by Mouw and Yoder (2010) and Devred et al. (2006, 2011). These models use the concentration of Chl$a$ calculated from satellite data and allow one to determine the absorption of particles in two size classes: small (<20 μm) and large (> 20 μm) particles.

Other studies reported by various authors concern the modeling or parameterization of light absorption by phytoplankton indirectly, on the basis of Diagnostic Pigment Analysis (DPA) (Vidussi et al., 2001; Uitz et al., 2006, 2008;

75 Brewin et al., 2010, 2012; Hirata et al., 2008, 2011), where three particle size classes are defined: picoplankton, nanoplankton, and microplankton. Various approaches to identify the size structure of phytoplankton populations from satellite data are detailed in the IOCCG report (2014).

Such models do not work for the Baltic Sea, which is a reservoir classified as optically complex (for the DPA method, the results are presented in Meler et al., 2020). The Baltic Sea is a semi-enclosed basin, shallow, characterized by low salinity

80 and a very large inflow of substances from land. This water basin is also characterized by specific optical properties, different from ocean waters (Kowalczuk et al., 2006, 2015; Meler et al. 2016 a, b, 2017, 2018; Woźniak et al., 2011, 2020, 2022). Therefore, most of the algorithms (mathematical formulas) used to interpret remote observation methods of marine and oceanic environments are not applicable to the Baltic Sea, as they do not take into account the specificity of its waters and hence are subject to large errors. They should be modified or replaced with new ones. For this purpose, *in situ* studies should be carried

85 out, which would allow to directly determine the light absorption coefficients not only by phytoplankton, but also by all particles and detritus in various size fractions.

The aim of our research was to investigate the variability of the spectra of the light absorption coefficients by different size fractions of suspended particles (a_p) present in the Baltic Sea, in the division into phytoplankton (a_ph) and detritus (a_d). It was carried out for four distinguished size classes: picoplankton (with diameters of 0.2-2 μm), ultraplankton (2-5 μm),

90 nanoplankton (5-20 μm) and microplankton (20-200 μm) according to the division proposed by Sieburth et al. (1978) and Ciotti et al. (2002). The specific objectives were: 1) to determine the contribution of size classes in the total light absorption by particles, phytoplankton and detritus, 2) to determine the average chlorophyll-specific and mass-specific light absorption coefficients, i.e., light absorption coefficients normalized to the concentration of Chl$a$ or the concentration of suspended particulate matter (SPM)) for distinguished size classes.

2 Materials and methods

2.1 Water samples

Seawater samples were collected in the southern part of the Baltic Sea, from December 2020 to October 2021. The dataset includes 22 sets of data collected during 3 research cruises on board the R/V *Oceania* (in February, April and September 2021) and 16 sets of data collected during field experiments on the most protruding part of the pier in Sopot (Poland). Figure 1 shows the location of the measurement stations. During the cruises, locations were selected to obtain the greatest possible diversity of waters in optical terms. Cyclical measurements on the Sopot pier were made monthly, from December 2020 to May 2021 and in October 2021, and every 7-14 days in the summer period from June to mid-September 2021. The basic characteristics of the water samples were measured (water transparency using the Secchi disk, temperature, and salinity). The seawater samples were fractionated according to the size of the suspended particles in the water in a specially designed filtration set through filters/filter meshes with different pore sizes (20 μm, 5 μm, 2 μm). Filtrates of fractions A, B, and C were obtained. The filtration set consisted of two PVC pipes with a diameter of 20 cm and a height of 38 cm and a diameter of 15 cm and a height of 38 cm, between which Teflon square plates 24x24 cm with hollow holes of 15 cm and 13 cm are placed on a metal mesh to allow free flow of water. A nylon mesh (HydroBios, 20 μm and 5 μm) with a size of 24x24 cm was placed on a plate, secured with a gasket, pressed against the second plate and filtration was carried out.
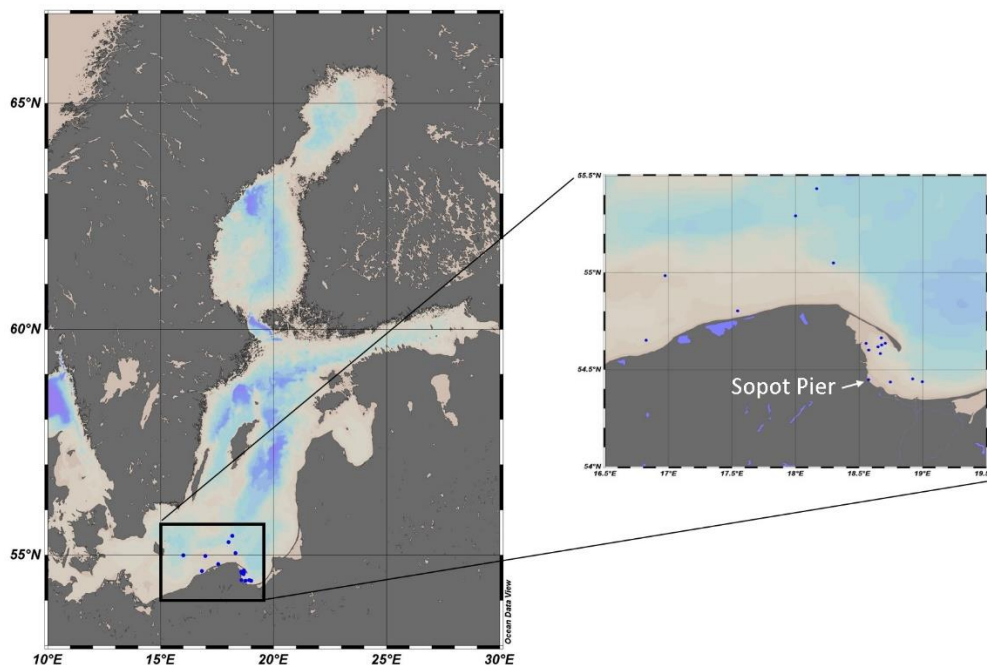
Figure 1: Location of measurement stations in the Baltic Sea.

At each location, 40 L to 100 L of surface seawater was collected and integrated into a large tank. 10 L-20 L of water was then extracted and treated as the original (unfiltered) seawater sample. The rest of the water from the integration tank was fractionated by particle size (similar to Koestner et al., 2019). First, the water was gravity filtered through a nylon mesh with 20 μm pores and filtrate of fraction A was obtained. 10 L to 20 L of fraction A was left/cast, and the rest was gravity filtered through a nylon mesh with pores of 5 μm and the filtrate of fraction B was obtained. After separation of the appropriate volume of water for fraction B, the rest of the water was filtered through membrane filters (hydrophilic polycarbonate membrane) Whatmann (Nulepore, 47 mm) or Millipore (Isopore, 47 mm) with pores of 2 μm (under pressure < 0.04 MPa) – the filtrate of fraction C was obtained. Despite the use of specialized nylon meshes with specific mesh sizes, it should be taken into account that filtration of water through them did not guarantee a perfect separation of particle size fractions. Single meshes were used multiple times, after being gently washed with detergent, then rinsed with deionized water, and dried. During the pouring of water, or subsequent washing or rinsing, the meshes could be deformed in any way, causing possible passage of particles with diameters larger than the mesh size to the next filtrate. Moreover, particles suspended in seawater do not have a perfectly spherical shape, this is just an assumption to simplify scientific considerations.

The original seawater samples and fractions A, B and C were filtered to determine the physicochemical parameters: coefficients of light absorption by all suspended particles ($a_p(\lambda)$, m^{-1}), detritus ($a_d(\lambda)$, m^{-1}) and phytoplankton ($a_{ph}(\lambda)$, m^{-1}), concentrations of Chl$a$ (mg m^{-3}) and concentrations of SPM (g m^{-3}) (including organic (POM) and inorganic (PIM) matter).

The values of individual biogeochemical and optical parameters in all distinguished size classes (micro-size, nano-size, ultra-size and pico-size) were determined as follows. The micro-size was determined by the difference of the original water sample and fraction A. The nano-size was determined by the difference of fraction A and fraction B; the ultra-size was determined from the difference of fraction B and fraction C, while the pico-size was determined from fraction C (the division of phytoplankton particles according to Ciotti et al., 2002).

There have been cases where 'fraction difference' has given a negative value. If the difference between the original water sample and fraction A was negative, it was assumed that the micro-size class was not present hence equal to zero. In this case, fraction A was treated as the value of the original sample. Similar assumptions were used when the differences between fraction A and fraction B or between fraction B and fraction C were negative. It was also assumed that the sum of individual parameters (light absorption coefficients, Chl$a$ and SPM concentrations) obtained for size classes should be equal to the parameters determined for the original, unfractionated seawater sample.

2.2 Absorption properties

Spectra of light absorption coefficients by particles suspended in seawater, $a_p(\lambda)$, and by detritus, $a_d(\lambda)$, (particles depigmented by the use of bleach, also called nonalgal particles in the literature), for the original samples and fractions A, B and C were measured using a Perkin-Elmer Lambda 650 spectrophotometer equipped with a 150 mm diameter integrating sphere (measurements inside the sphere). Seawater samples for these analyzes were obtained by filtering small volumes of seawater (from 40 mL for original water samples to 1000 mL for fraction C) through Whatman filters (GF/F, 25 mm). Filters with

145 suspension were stored in liquid nitrogen in a dewar flask and then in a freezer (approx. -20^{0}C) until analyses. Spectrophotometric measurements were performed using a holder in the form of a clip holding a filter with suspension, placed inside the integrating sphere (Stramski et al. 2015, Woźniak et al., 2022). Measurements were performed in the spectral range of 290-860 nm and were carried out in two configurations: for filters with a suspension and for the same filters bleached with a 2% solution of sodium hypochlorite NaClO$_2$ (Meler et al., 2020). Two repetitions were made and averaged. Such spectra

150 were corrected with use of the averaged reference spectra obtained by the measurements on filters through which 30 mL of particle-free seawater was passed. To take into account the lengthening of the optical path of the light falling on the filter with suspension in relation to the same suspension in water, the so-called beta factor was calculated following Stramski et al. (2015). The light absorption coefficients by particles and detritus were determined. From their difference, the light absorption coefficients of phytoplankton ($a_{ph}(\lambda)$) were determined.

155   The spectra of the light absorption coefficients of the chromophoric dissolved organic matter, $a_{CDOM}(\lambda)$ (m^{-1}), were determined spectrophotometrically using a Perkin-Elmer Lambda 650 spectrophotometer. The original seawater samples were first filtered through Whatman filters (GF/F, 47 mm) with nominal pores of 0.7 μm, and then through Sartorius acetone membrane filters (47mm) with pores of 0.2 μm. The filtrate prepared in this way was stored in amber glass bottles in a refrigerator (+4 ^{0}C) until further analysis. Measurements were carried out in the spectral range of 200-700 nm in quartz cuvettes

160 with a 10 cm optical path length. Deionized water was used as a reference. The optical density OD(λ) was converted to CDOM absorption by multiplying OD(λ) by a factor of 2.303 and then dividing by the path length l (m). Finally, the spectra were corrected for residual scattering according to Kowalczuk et al. (2006). The slope coefficients of the light absorption by CDOM in the spectral range of 300-600 nm (S$_{300-600}$, m^{-1}) were calculated using the nonlinear least squares fitting that employed the Trust-Region algorithm implemented in Matlab R2013 (Kowalczuk et al., 2006; Stedmon et al., 2000).

2.3 Quantities characterizing suspended particulate matter

165

The concentrations of suspended particulate matter (SPM, g m^{-3}), and its organic (POM) and inorganic (PIM) fractions were determined by the gravimetric method and the loss-on-ignition technique (Woźniak et al., 2018; Pearlman et al., 1995). Seawater samples for these analyzes were obtained by filtering seawater (original and fractions A, B, and C) through previously prepared Whatman filters (GF/F, 25 mm). These filters were first combusted at 450 ^{0}C for 4.5 h, then rinsed with 0.5 L of pure

170 deionized water and dried for 24 h at 60 ^{0}C. After another 24 hours in the desiccator, the filters were weighed and labeled accordingly. 150 to 2800 mL of seawater was filtered through the filters, depending on the concentration of suspension particles, and then rinsed with 30 mL of clean, deionized water to remove salts from the surface of the suspension on the filter. Filters with suspension were dried at 60 ^{0}C for 24 h and stored in a freezer until analysis. In the laboratory, the filters were dried again at 60 ^{0}C for 24 h, stored in a desiccator for another 24 h, and then weighed. In this way, the SPM value was

175 obtained. In the next step, the filters were combusted at 450 ^{0}C for 4.5 h and weighed. The difference in the weights of the filters with and without the suspension allowed to determination of the SPM concentrations, while the difference in the weights of the filters with the suspension before and after combustion allowed to determination of the POM concentrations. The PIM

was calculated from the difference of SPM and POM. The SPM and POM values were also corrected with use of reference filters rinsed with 30 mL of pure deionized water and subjected to the same procedures as the filters with suspension.

180   The concentrations of chlorophyll *a* (Chl*a*, mg m^{-3}) were determined by the spectrophotometric method (Lorenzen, 1967). Seawater (original and fractions A, B, and C) was filtered through Whatman filters (GF/F, 47 mm) - from 0.5 L to 7.5 L. The filters were put into liquid nitrogen and then stored in a freezer until analysis. After thawing, the pigments contained in the suspension collected on the filters were extracted in 96% ethanol (8 mL) at room temperature for 24 h (Wintermans and De Mots, 1965; Marker et al., 1980). The extract was centrifuged for 15 minutes and then measurements were made using a

185   Perkin-Elmer Lambda 650 spectrophotometer in 2 cm cuvettes. The 96% ethanol was used as a reference). Chl*a* concentrations were calculated according to the formula of Stricland and Parsons (1972):

$$Chla(\lambda) = \frac{10^3 \cdot e \cdot (OD(665) - OD(750))}{83 \cdot l \cdot v},\tag{1}$$

where *e* is the volume of ethanol (cm^3), OD(665) and OD(750) are the optical density at 665 nm and 750 nm respectively, after correction for blank ethanol, 83 (L g^{-1} cm^{-1}) is the chlorophyll-specific absorption coefficient for ethanol, *l* is the length of the

190   cuvette (cm), *v* is the volume of filtered seawater (L).

3 Results and discussion

3.1 Variability of the biogeochemical properties of suspended matter

The analyzed dataset is characterized by significant variability of biogeochemical parameters defining suspended matter in seawater, both for original water samples and divided into size classes micro-size (20-200 μm), nano-size (5-20 μm), ultra-

195   size (2-5 μm) and pico-size (<2 μm). Table 1 summarizes this variability in detail and presents mean values with standard deviations (SD), and minimum and maximum values. Within 10 months of empirical data collection, a wide variability of SPM concentrations from 0.39 to 15.24 g m^{-3} and Chl*a* concentrations from 0.18 to 6.85 mg m^{-3} was obtained for the original water samples. Figure 2a shows the average contribution of suspended matter in a given size class to total suspended matter for individual samples. It should be noted that in the total SPM in given size fractions (further referred to as micro-, nano-,

200   ultra- and picoplankton for simplicity) there are not only phytoplankton cells, but also detritus and mineral particles. For the first 14 samples, it was not possible to separate the ultra and picoplankton fractions, because the amount of suspension of 2-5 μm clogged the membrane filters. For time reasons related to the sampling and filtering of large volumes of seawater for the determination of SPM (3-replicants) and Chl*a*, separation of the ultra and picoplankton fractions was abandoned for these 14 samples. In Figure 2, this 0.2-5 μm fraction is treated as one and marked with a dark gray dashed area.

205   The average contribution of the SPM in a given size class in the total SPM in the collected data set is similar in the pico-size, ultra-size and nano-size classes of particles - always above 25 %, while the average contribution of micro particles was about 20 %. The variability of particles defined as microplankton was 0-59 %, but a contribution in the total SPM greater than 40 % was observed only for 3 cases (for samples collected at the pier in Sopot - 2 cases in summer during phytoplankton bloom and 1 case in winter). The contribution of nano-particles varied in the range of 0-67 % (contribution > 40% was

210 observed for 9 cases), ultra-particles in the range of 1-50 % (contribution > 40% was observed for 5 cases), and pico-particles
in the range of 5-51 % (contribution > 40% was observed for 7 cases). No similar studies have been reported in the available
literature so far. Fractionation based on the size of the particles suspended in the water column was carried out for completely
different particle size ranges (<50 μm and >50 μm) and was most often associated with geotrace studies, in which the chemical
composition of the suspension was determined (e.g., Lam et al. , 2015, 2018; Xiang and Lam, 2020; Yigiterhan et al., 2020).

215 However, in the work of Mohammadpour et al. (2017) optical properties of SPM size fractions in littoral waters of Quebec
were studied, but for size classes 0.2-0.4 μm, 0.4-0.7 μm, 0.7-10 μm and > 10 μm. The contribution of particles with sizes >
10 μm did not exceed 17 %.

Table 1: Variability of parameters characterizing suspended matter in seawater (mean ± standard deviation (SD), and range of variation)

quantity (n=38)	SPM [g m^{-3}]	POM [g m^{-3}]	PIM [g m^{-3}]	Chl$a$ [mg m^{-3}]	POM/SPM	Chl$a$/SPM
original samples (all particles, unfiltered)						
average ± SD	2.35 ± 2.83	1.10 ± 0.93	1.25 ± 2.02	1.75 ± 1.70	0.58 ± 0.21	0.001 ± 0.0007
min - max	0.38-15.24	0.20-4.54	0-10.70	0.18-6.85	0.28-1	0.0002-0.0032
Micro particles (20-200 μm)						
average ± SD	0.58 ± 1.49	0.19 ± 0.31	0.39 ± 1.20	0.29 ± 0.45	0.53 ± 0.33	0.0011 ± 0.0015
min - max	0-8.97	0-1.75	0-7.22	0-1.87	0-1	0-0.0066
Nano particles (5-20 μm)						
average ± SD	0.71 ± 0.1	0.31 ± 0.33	0.40 ± 0.70	0.47 ± 1.02	0.59 ± 0.22	0.0007 ± 0.0008
min - max	0-4.95	0-1.57	0-3.38	0-5.07	0-1	0-0.0029
Ultra praticles (2-5 μm)						
average ± SD	0.55 ± 0.57	0.34 ± 0.28	0.22 ± 0.36	0.67 ± 0.62	0.87 ± 0.82	0.0037 ± 0.0104
min - max	0.01-2.34	0.02-1.01	0-1.59	0.06-2.85	0.32-4.62	0.0003-0.0521
Nano+ultra particles (2-20 μm)						
average ± SD	1.11 ± 1.22	0.63 ± 0.46	0.49 ± 0.82	0.99 ± 1.01	0.69 ± 0.21	0.0011 ± 0.0007
min - max	0.28-5.49	0.14-2.15	0.0001-3.34	0-4.91	0.30-1	0-0.0027
Pico particles (< 2 μm)						
average ± SD	0.43 ± 0.29	0.32 ± 0.28	0.10 ± 0.07	0.57 ± 0.28	0.63 ± 0.31	0.0026 ± 0.0035
min - max	0.06-1.19	0-1.10	0-0.21	0.04-0.95	0-1	0.0001-0.0136

220   In the case of chlorophyll *a*, the average contribution in a given size class to the total concentration of Ch*la* is the highest for pico-particles (35 %) and ultra-particles (35 %), while the average contribution of Ch*la* in nano and micro-particle classes is about 15 % each. The range of variability of the contributions of individual size classes in the total Ch*la* changed as follows: micro-particles from 0 to 53 %, nano particles from 0 to 76 %, ultra-particles from 11 to 86 % and pico-particles from 5 to 66 %.

225   Reported by Maranon et al. (2001) contributions of Ch*la* in fractions up to the total concentration of Ch*la* (integrated for the water column 0-200 m) in the waters of the Atlantic Ocean showed that in most data the contribution of picoplankton was 60-80 % (average 61 %), nanoplankton (including ultraplankton) was approximately 20 % to 30 % (average 29 %) (from low-production regions to temperate regions), while the contribution of microplankton varied from < 10 % to 20 % (the share was low in most cases and increased to 20 % in upwelling areas and moderate, especially in spring) (average 9 %). Deng et al.

230 (2022) presented results for data from the southern part of the China Sea from the surface layer, where the average contribution of picoplankton was 81 %, nanoplankton (including ultraplankton) 12 % and microplankton 7 %. In turn, Decembrini et al. (2014) for the Magellan Strait investigated the seasonal variability of the contributions of fractions in total Ch*la* integrated for a depth of 0-50 m. For the spring season, the contribution of picoplankton in total Ch*la* was on average 12 %, and the micro+nano fraction was 88 %. In the summer season, the contribution of picoplankton was on average 60 %, micro+nano 40

235 %. In late summer and early autumn, the average contribution of picoplankton was 47 % and micro+nano 53 %. Saggiomo et al. (1994) for austral summer (February–March 1991), in the Strait of Magellan, reported that the most important characteristic identified for this area was the confinement of the microplankton fraction to the external parts of the Strait and the rather uniform dimensional structure of the phytoplankton communities (< 5 μm) within the internal sectors. In particular, the nanoplankton fraction (2-10 μm) comprised 33 %, while the picoplankton one (0.5-2 μm) represented 62 % of the total.

240 Cermeno et al. (2005) studied the photosynthetic efficiency of fractionated phytoplankton in the Ria de Vigo (Iberian Penisula). The contribution of fractions with sizes < 5 μm was on average 46 %, fractions with sizes 5-20 μm and > 20 μm were 27 % each, in the total Ch*la* integrated in the euphotic zone (0-20 m). All the cases of phytoplankton fractionated by size described above concern studies related to primary production. The data presented in this paper do not differ from those reported in the literature. By comparison of the above data, it can be seen that the percentage contribution of individual size fractions to the

245 total concentration of Ch*la* is not a constant value, but changes over time and space.

      The POM/SPM ratio expresses the proportion of organic matter in the total mass of suspended solids and can vary from 0 (purely mineral suspension) to 1 (100% organic suspension). The dataset was divided into 5 classes, reflecting the change in suspension composition in the analyzed dataset. POM/SPM for the original samples ranged from 0.28 to 1 (Figure 3). Analyzes of the POM/SPM ratio in individual size classes show similar variability. It can be seen that with an increase in the

250 SPM value, the proportion of organic particles in the suspension decreases. The exception is the variation of POM/SPM for ultra and pico particles. Here, the contribution of organic matter increases with increasing SPM. The average contribution of POM/SPM was about 60% for the entire suspension, as well as for the micro and nano particle classes. On the other hand, for classes of particles with diameters below 5 μm, the average contribution of POM/SPM was higher, > 70%.
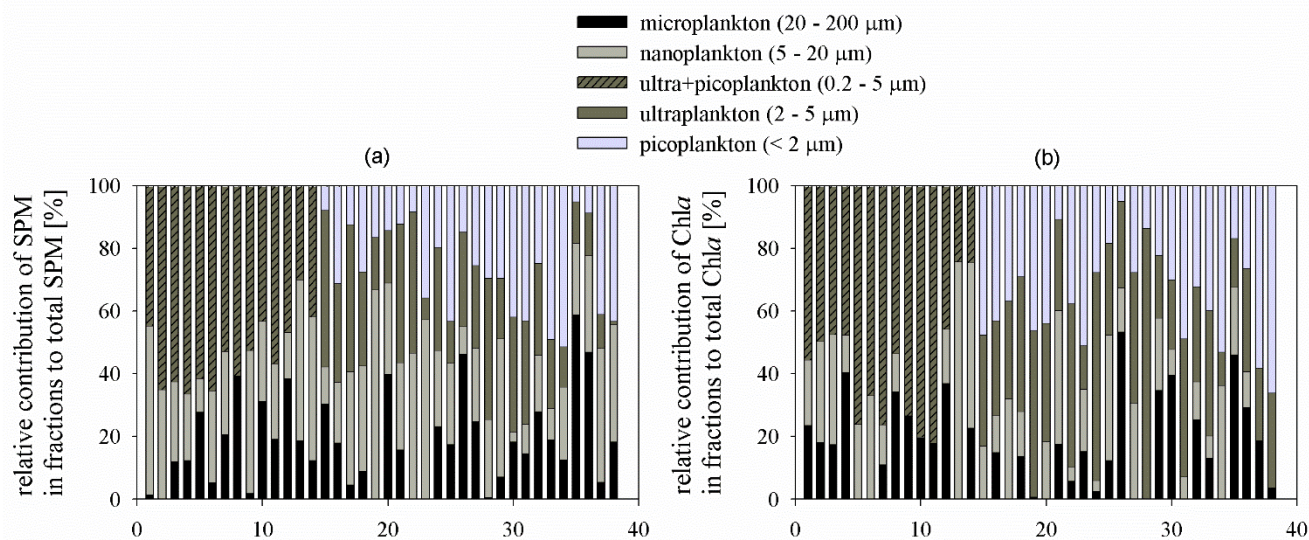
Figure 2: Relative contribution of (a) SPM in the selected fraction to the total SPM, and (b) Chl*a* in the selected fractions to the total Chl*a*.

In the works of Woźniak and Meler (2020) and Woźniak et al. (2022) on the study of the optical properties of the waters of the Baltic Sea (conducted in the period 2017-2020), the presented POM/SPM ratios were characterized by similar values. The average POM/SPM was 61% and 62%, respectively. In previous studies, the average POM/SPM for the Baltic Sea was 80% (Woźniak et al., 2011 - for the period 2006-2009) and 76% (Meler et al., 2016 a, b - for the period 2006-2012). Long-term variability from previous years indicated a higher proportion of organic particles in the total suspension, while data from 2017-2021 may indicate that the proportion of detrital and mineral particles in the particle composition increased. However, this may be due to the increased number of stations located in the coastal waters zone in the total database. This, in turn, is caused by the variability of the weather (change in climatic conditions). In recent years, optical cruises, which have been taking place more or less at similar times of the year for 20 years, are characterized by more windy weather, which results in sailing closer to the coastal zone (there is less data from open waters), and therefore there is a greater proportion of particles flowing from land and/or lifted from the bottom, as a result of stormy weather.
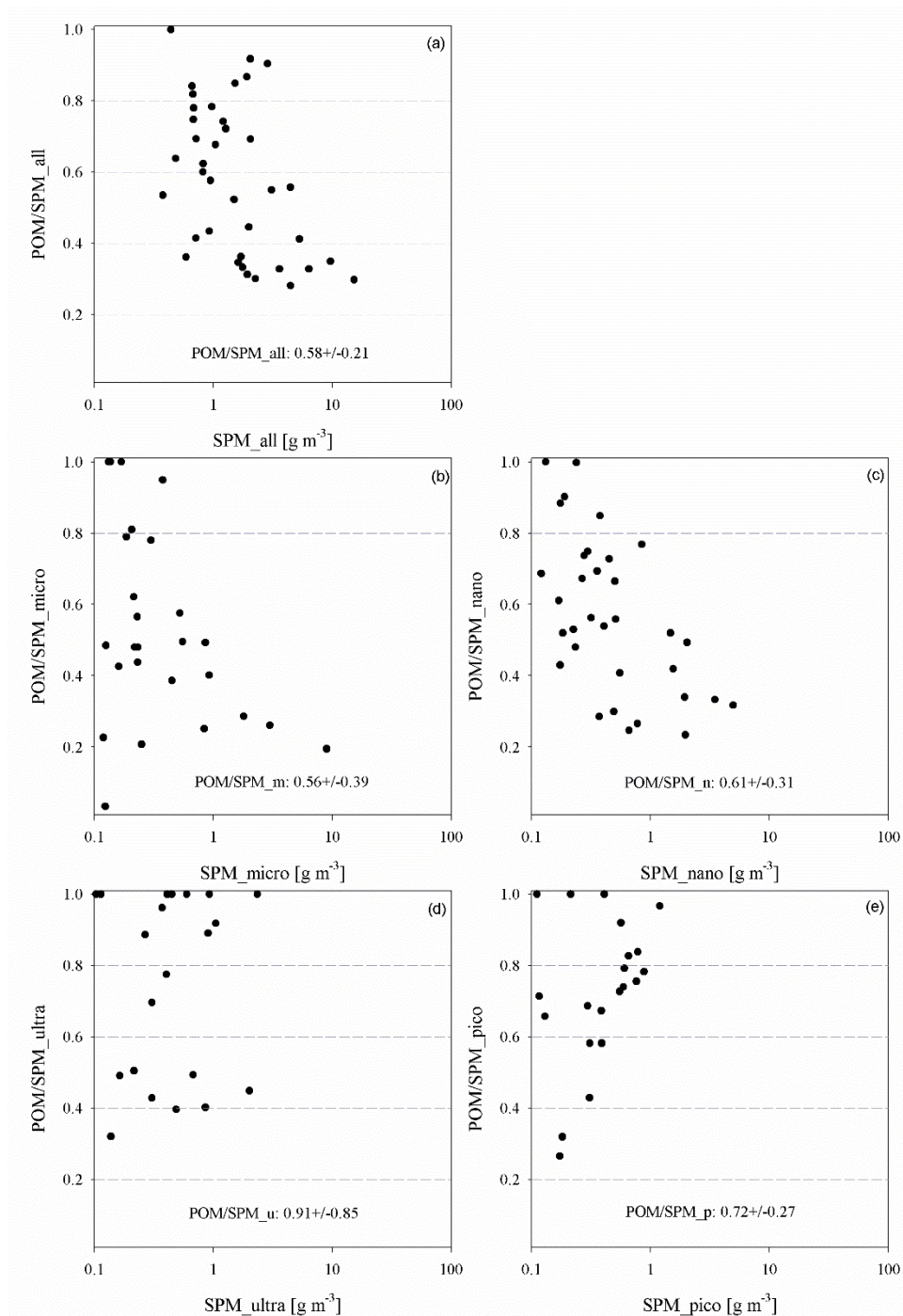
Figure 3: Relationships between the POM/SPM composition ratio and the SPM concentration for the original water
270 **samples and in the micro, nano, ultra and pico size classes. Mean values ± standard deviation are shown in the graph.**

The Chl$a$/SPM ratio, which is an indicator of the variability of the photosynthetic contribution of live plankton in the entire suspension population, ranges from $6*10^{-4}$ to $4.1*10^{-3}$ for the original samples. For earlier studies of the Baltic Sea, Woźniak et al. (2022) had a variation of $1*10^{-4}$ to $9.3*10^{-3}$. In individual size classes, the variability is similar and with increasing proportion of live phytoplankton in the entire suspension, the proportion of POM/SPM increases. For micro-size

275   Chl$a$/SPM it varies from $6*10^{-5}$ to $9.5*10^{-3}$, for nano-size from $9*10^{-6}$ to $4.6*10^{-3}$, ultra-size from $6*10^{-4}$ to $6*10^{-3}$, and pico-size from $3*10^{-4}$ to $6.4*10^{-3}$.

3.2 Variability of absorption properties of suspended and dissolved matter (all particles, detritus, phytoplankton and CDOM)

Figure 4 shows the spectra of light absorption coefficients for all suspended particles, detritus, and phytoplankton determined
280   in the analyzed dataset. The left panel shows the variability of these coefficients for the original unfractionated seawater samples. The right panel shows the variability of $a_p(\lambda)$, $a_d(\lambda)$ and $a_{ph}(\lambda)$, calculated for the micro, nano, ultra and pico-size classes. Variability of two orders of magnitude was recorded for the original water samples. In the case of the micro, nano and ultra-size classes, this variability was greater than two orders of magnitude, whereas for the pico class it was slightly more than one order of magnitude.

285   Figure 4g shows the spectra of the coefficients of light absorption by chromophoric dissolved organic matter (CDOM) calculated for the analyzed dataset. The average slope of the spectra ($S_{300-600}$) determined for the 300-600 nm range was 0.022 ± 0.001 m^{-1}. The light absorption coefficients: $a_{ph}(\lambda)$, $a_d(\lambda)$ and $a_{CDOM}(\lambda)$, allowed one to calculate the light absorption budget for the selected wavelength of 443 nm (Figure 4h). For the analyzed dataset, the average contribution of light absorption by phytoplankton was 29 % $\pm$ 14 %, the average contribution of light absorption by detritus was 19 % $\pm$ 9 % (the average
290   proportion of $a_{ph}(443)$, $a_d(443)$ and $a_{CDOM}(443)$ is marked with a red triangle). The greatest contribution to the total light absorption was made by CDOM: 52 % $\pm$ 20 %. Similar analyzes were carried out by Woźniak et al. (2011) and reported for the wavelength of 440 nm the average contribution were: $(a_{ph}(440) + a_d(440)) - 45$ % and $a_{CDOM}(440) - 55$ %.
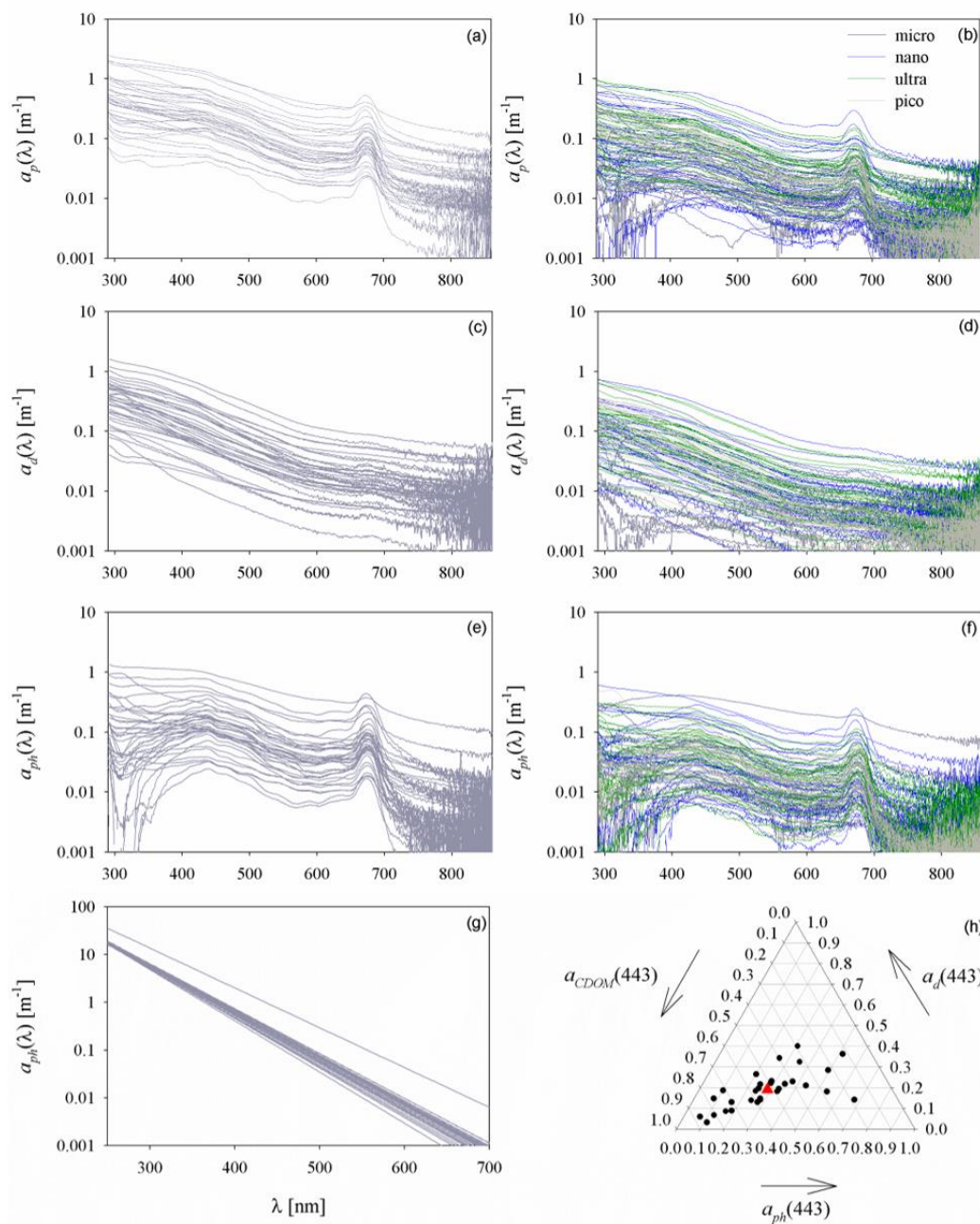
Figure 4: Spectra of light absorption coefficients by particles suspended in seawater ($a_p(\lambda)$), detritus ($a_d(\lambda)$) and phytoplankton ($a_{ph}(\lambda)$) for original, unfractionated water samples - left panel (a, c, e) and calculated for micro, nano, ultra and pico-size classes - right panel (b, d, f); spectra of CDOM light absorption coefficients ($a_{CDOM}(\lambda)$) (g) and ternary plot showing the light absorption budget for the 443 nm wavelength in the analyzed dataset (h) (the red triangle shows the average contribution of individual absorption coefficients to the total light absorption).

3.3 Variability of light absorption coefficients vs Chl*a* and SPM

300 In this work, we focus on showing the variability of light absorption coefficients by size fractions of particles suspended in water. Therefore, it is important to show how these different size fractions depend on the concentration of Chl*a* and SPM, which are the basic characteristics of these suspensions.

Figure 5 presents the light absorption coefficients of all particles suspended in seawater for a wavelength of 443 nm depending on the concentration of Chl*a* and SPM, for the original (unfractionated) seawater samples and for the micro, nano,

305 ultra and pico-size classes. It can be seen that the better relationships $a_{p,i}(443)$ (where *i* means: all – all particles, m – particles of the micro-size class: 20-200 μm, n – particles of the nano class: 5-20 μm, u – from the ultra class: 2-5 μm, and p - particles of the pico class: < 2 μm) were obtained from the SPM than Chl*a* for all coefficients. The coefficient of determination, R^2, for the dependence of $a_{p,all}(443)$ vs Chl*a* was 0.74 and for the dependence of $a_{p,all}(443)$ vs SPM – 0.85. For the micro, nano and ultra-size classes, R^2 for both dependencies was 0.46 and 0.81, 0.73 and 0.88, 0.55 and 0.67, respectively. Only the

310 dependencies $a_{p,p}(443)$ vs Chl*a* and vs SPM had comparable R^2: 0.48 and 0.45. The original relationships (unfiltered samples) were slightly different in Woźniak et al. (2011). There, for the wavelength of 440 nm, the coefficient of determination for the dependence $a_{p,all}(440)$ vs Chl*a* was 0.73, and for the dependence $a_p(440)$ vs SPM - 0.53.

Figure 6 shows the light absorption coefficients by detritus for a wavelength of 443 nm depending on the Chl*a* and SPM concentrations for the original seawater samples and for the micro, nano, ultra and pico size classes. As in the case of

315 $a_{p,i}(443)$, it can also be seen that in most cases better relationships were obtained with the SPM than with the Chl*a*. In the case of size classes, the coefficients of determination R^2 for the dependence $a_{d,i}(443)$ vs Chl*a* and SPM were, respectively: micro - 0.58 and 0.79, nano - 0.54 and 0.87, ultra - 0.38 and 0.61, pico - 0.05 and 0.51. The exception is the dependence of $a_{d,all}(443)$ vs Chl*a* and SPM, where R^2 was 0.61 and 0.50, respectively. In the case of the coefficient $a_{d,all}(443)$ for the Baltic Sea, it has been already shown that the dependence on SPM is better than the dependence on Chl*a* (Woźniak et al., 2011; Meler et al.,

320 2017).

Figure 7 shows the relationships for the light absorption coefficients by phytoplankton for the original water samples and for the size classes. It is somewhat surprising that for the analyzed dataset it was also observed that the coefficients $a_{ph,i}(443)$ correlate better with the SPM than with the Chl*a*. An exception is the dependence for picoplankton, where the R^2 coefficient for the dependence $a_{ph,p}(443)$ vs Chl*a* was 0.66 and for SPM only 0.15. In the remaining cases, R^2 for dependence

325 $a_{ph,i}(443)$ vs SPM was higher than for $a_{ph,i}(443)$ vs Chl*a* and ranged from approximately 0.02 to 0.29. Comparing these relationships with those obtained by Woźniak et al. (2022), shown for a wavelength of 440 nm, it can be seen that also in this case the a_{ph} vs SPM relationships have higher determination coefficients R^2 than the a_{ph} vs Chl*a* relationships, 0.86 and 0.82, respectively.
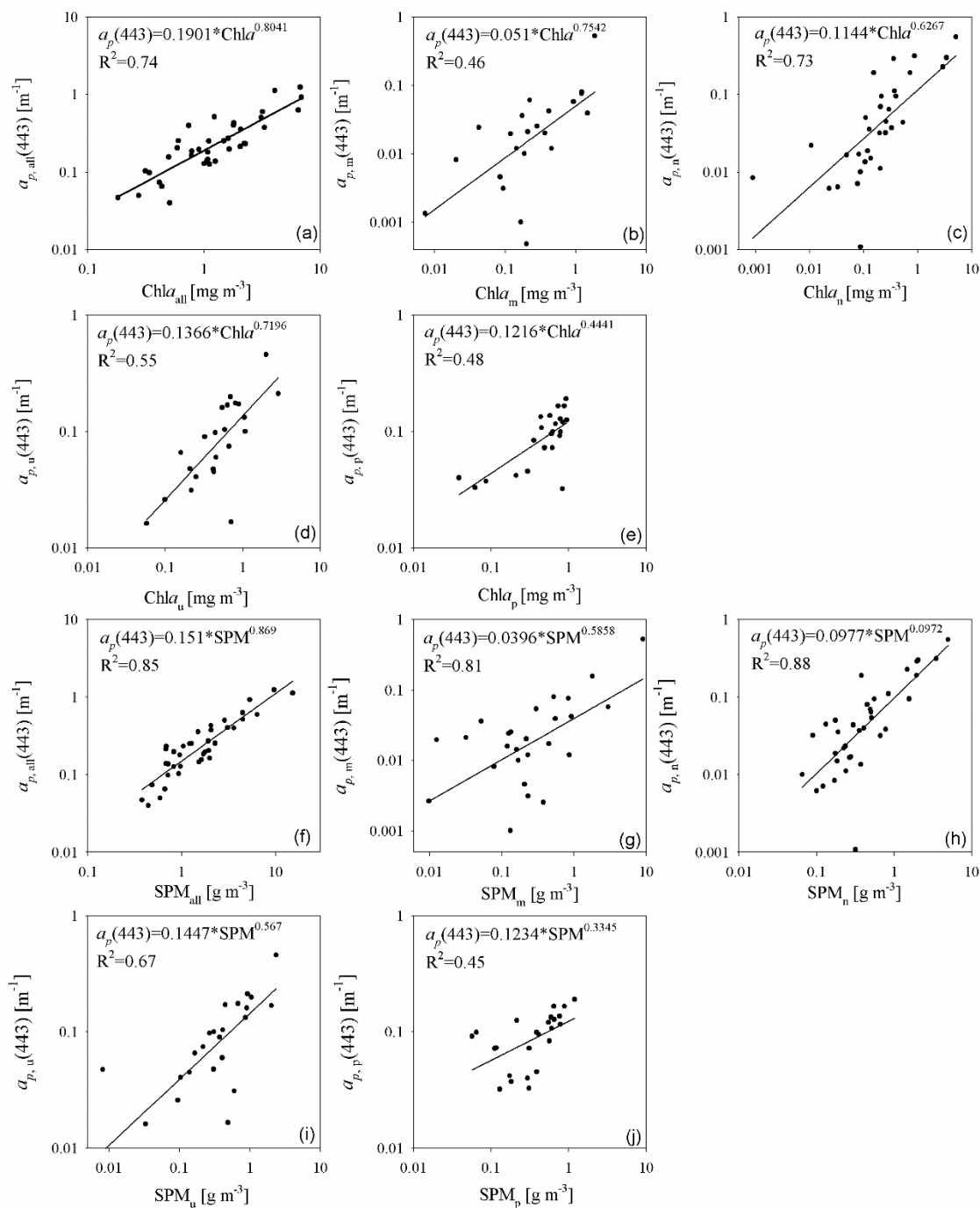
Figure 5: Relationships of the light absorption coefficients by all unfractionated particles (a, f) and in size classes: micro (b, g), nano (c, h), ultra (d, i) and pico (e, j) from the Chl*a* (a-e) and SPM (f-j), for the selected wavelength of 443 nm. Note that graphs have different axis scales.
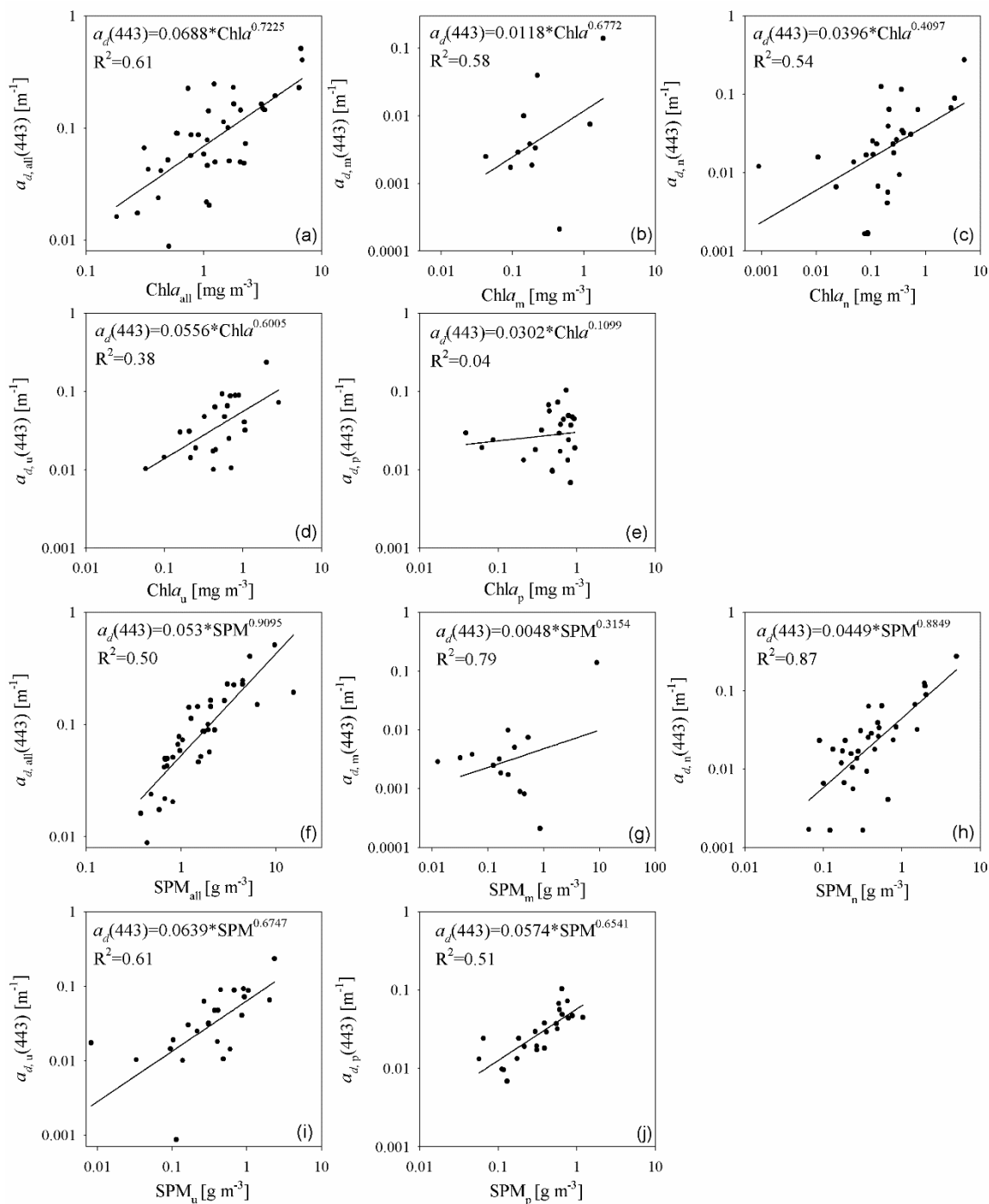
Figure 6: Relationships of the light absorption coefficients by all unfractionated detritus (a, f) and in size classes: micro (b, g), nano (c, h), ultra (d, i) and pico (e, j) from the Chl*a* (a-e) and SPM (f-j), for the selected wavelength of 443 nm. Note that graphs have different axis scales.

335
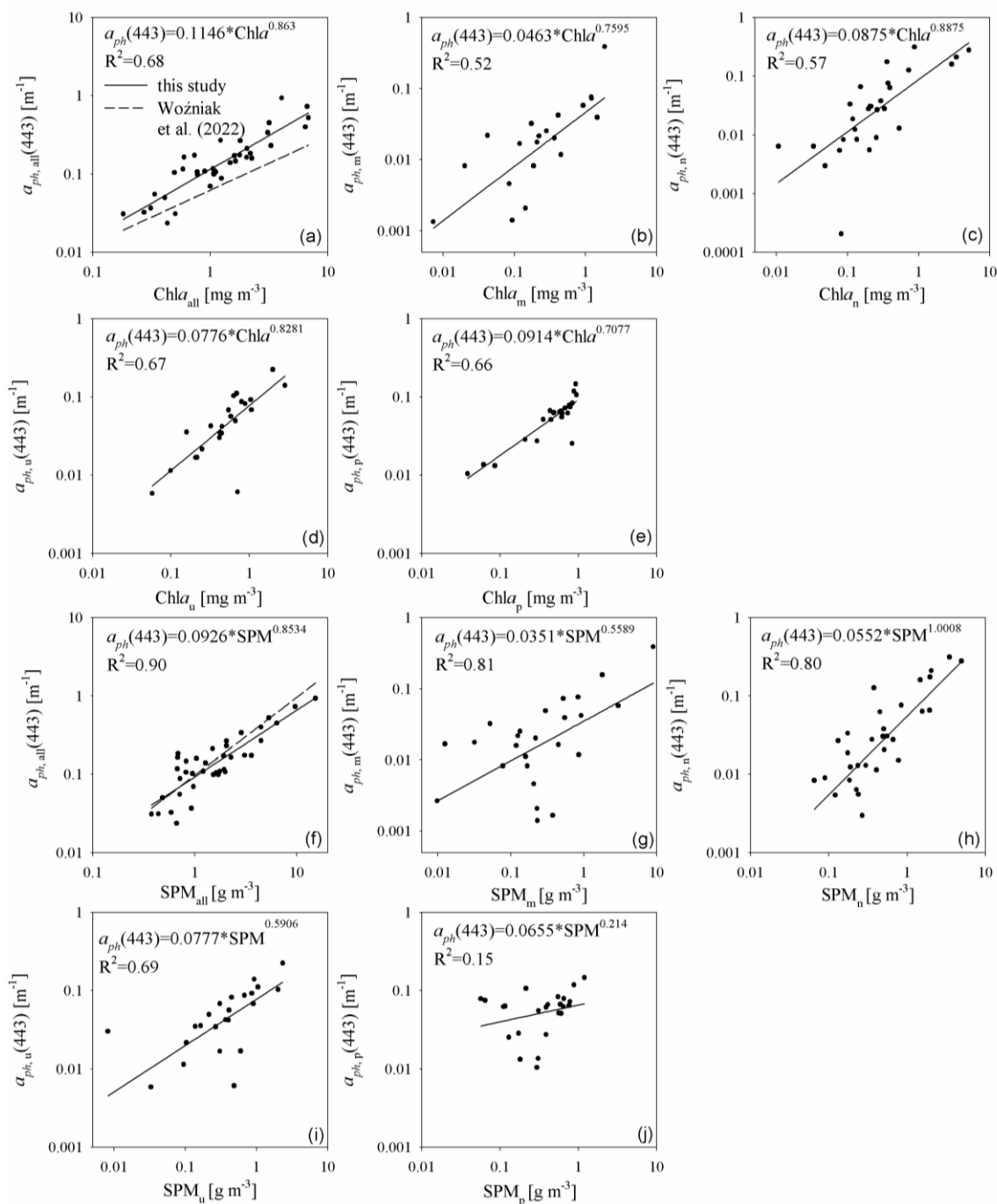
Figure 7: Relationships of the light absorption coefficients by all unfractionated phytoplankton (a, f) and in size classes: micro (b, g), nano (c, h), ultra (d, i) and pico (e, j) from the Chl*a* (a-e) and SPM (f-j), for the selected wavelength of 443 nm. Note that graphs have different axis scales.

340

3.4 Contribution of size classes to the total light absorption by all particles, detritus and phytoplankton for the wavelength of 443 nm

Measurements of the light absorption coefficients by particles, including detritus and phytoplankton, provided information on the contribution of the particle size classes (micro, nano, ultra and pico) to the total light absorption coefficients. Table 2

345 contains such contributions in our dataset divided into 3 size classes according to Sieburth et al. (1978): micro i.e. large particles (20-200 µm), nano-particles (containing the ultra fraction - 2-20 µm) and pico-particles (<2 µm). The largest contribution has medium particles with sizes from 2 to 20 µm - for each case, on average above 50 %. The small particles in the total absorptions had an average contribution of about 40 %. The rest was due to the contribution of large particles, about 5-10 % on average. The contribution of particle size classes to total absorption is also illustrated in Figure 8 a, c, e. If we consider the division of

350 particles into 4 size classes (according to Ciotti et al., 2002), it can be seen that in the total light absorption by particles, detritus or phytoplankton, particles with sizes < 5 µm - i.e. pico-particles and ultra-particles, had the largest contributions (on average about 38% and 31%). Particles with a size of 5-20 µm accounted for approximately 20% of all particles and phytoplankton, and 29% of the detritus. The proportion of large particles remained unchanged (Table 3). Graphically, the contribution of size classes to total absorption is illustrated in Figure 8 b, d, f.

355 To show the contribution of phytoplankton to the light absorption by all particles, the aph(443)/ap(443) ratio was analyzed for the original samples and in size classes. The average $a_{ph}(443)/a_p(443)$ for unfractionated samples was 0.62 ± 0.12. In the case of the micro size class, the average $a_{ph}(443)/a_p(443)$ ratio was 0.83 ± 0.26, in the nano class - 0.50 ± 0.29, and in the ultra and pico classes - 0.53 ± 0.12 and 0.60 ± 0.16, respectively. Thus, it can be seen that in the analyzed data set, the proportion of phytoplankton absorption in total absorption by all suspended particles was significant. However, in the case of

360 nano and ultra-size classes, there are many cases where detritus has a dominant contribution in light absorption.

Table 2: Contributions of particles from the micro, nano+ultra, pico-size classes to the total light absorption by particles, detritus and phytoplankton for a wavelength of 443 nm (n=38). The mean values ± standard deviation (SD) and the variability range are given.

	$a_{p,micro}/a_p$	$a_{p,nano+ultra}/a_p$	$a_{p,pico}/a_p$
average ± SD	0.07± 0.10	0.56 ± 0.13	0.38 ± 0.14
min - max	0-0.46	0-0.89	0.10-0.58
	$a_{d,micro}/a_d$	$a_{d,nano+ultra}/a_d$	$a_{d,pico}/a_d$
average ± SD	0.04 ± 0.12	0.60 ± 0.17	0.36 ± 0.11
min - max	0-0.72	0.04-1	0.09-0.56
	$a_{ph,micro}/a_{ph}$	$a_{ph,nano+ultra}/a_{ph}$	$a_{ph,pico}/a_{ph}$
average ± SD	0.10 ± 0.12	0.51 ± 0.16	0.39± 0.17
min - max	0-0.42	0.12-0.84	0.07-0.63
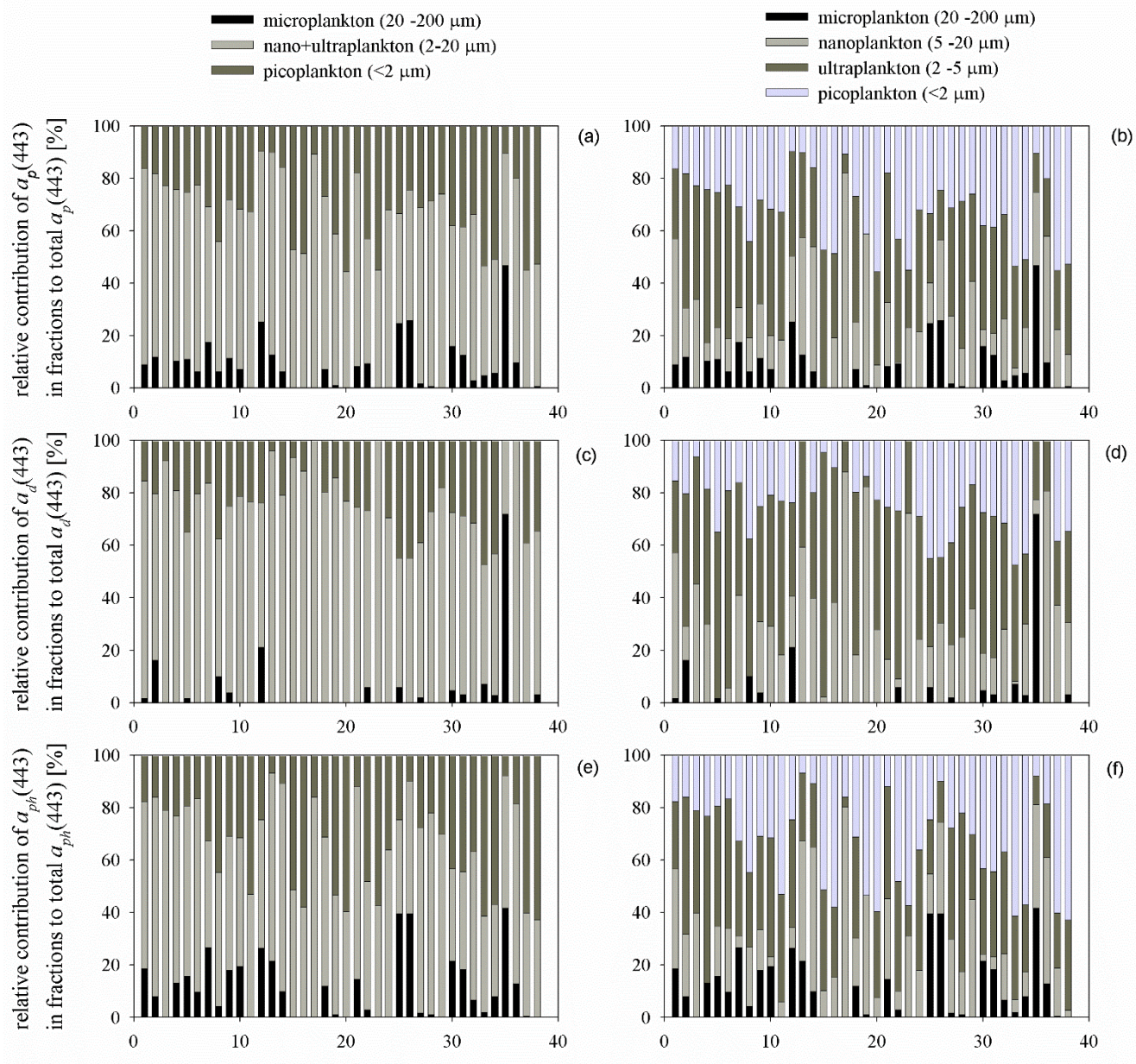
Figure 8: Contribution of particles from size classes in the total light absorption by all particles, detritus and phytoplankton according to the classic division into three size classes according to Sieburth et al. (1978) (micro-, nano-+ultra-, pico-particles) - left panel: (a, c, e) and by division into 4 size classes according to Ciotti et al. (2002) (micro-, nano-, ultra- and pico-particles) - right panel: (b, d, f).

370 **Table 3: Contributions of micro, nano, ultra and pico-size classes to the total light absorption by particles, detritus and phytoplankton for the wavelength of 443 nm (n=38). The mean values ± standard deviation (SD) and the variability range are given.**

	$a_{p,micro}/a_p$	$a_{p,nano}/a_p$	$a_{p,ultra}/a_p$	$a_{p,pico}/a_p$
average ± SD	0.07± 0.10	0.23 ± 0.17	0.33 ± 0.14	0.38 ± 0.14
min - max	0-0.46	0-0.82	0-0.59	0.10-0.58

	$a_{d,micro}/a_d$	$a_{d,nano}/a_d$	$a_{d,ultra}/a_d$	$a_{d,pico}/a_d$
average ± SD	0.04 ± 0.12	0.29 ± 0.22	0.31 ± 0.16	0.36 ± 0.11
min - max	0-0.72	0-0.87	0.04-0.93	0.09-0.56

	$a_{ph,micro}/a_{ph}$	$a_{ph,nano}/a_{ph}$	$a_{ph,ultra}/a_{ph}$	$a_{ph,pico}/a_{ph}$
average ± SD	0.10 ± 0.12	0.20 ± 0.14	0.31 ± 0.14	0.39± 0.17
min - max	0-0.42	0-0.80	0.12-0.64	0.07-0.63

3.5 Average specific light absorption coefficients of particles for distinguished size classes

The conducted analyzes allowed one to determine the average values of chlorophyll-specific light absorption coefficients by
375 particles, detritus, and phytoplankton in size classes. Such average values are often sought because they allow for a simple description of the relationship between biogeochemical and optical quantities. The averages were determined for the data that met the condition of the so-called fraction dominance (Ciotti et al., 2002; Kheireddine et al., 2018), where the ratio of Chl$a$_fraction to Chl$a$ concentrations for the original sample was greater than 40% for one size classes. In the event that 2 fractions met this condition simultaneously, the following condition had to be met: the Chl$a$_fraction/Chl$a$ ratio had to be
380 greater than 50%. To determine the average values of the mass-specific light absorption coefficients a_p, a_d, and a_{ph}, a similar SPM_fraction dominance criterion to the SPM of the original sample was used. The results are shown in Figure 9 for the classic division into three size classes: micro-size (20-200 μm) - large particles, nano+ultra-size (2-20 μm) - medium particles and pico-size (<2 μm) - small particles. The left panel shows the chlorophyll-specific coefficients $a_p^{(Chla)}(\lambda)$, $a_d^{(Chla)}(\lambda)$ and $a_{ph}^{(Chla)}(\lambda)$, while the right panel shows the mass-specific coefficients $a_p^{(SPM)}(\lambda)$, $a_d^{(SPM)}(\lambda)$ and $a_{ph}^{(SPM)}(\lambda)$. The average $a_p^{(Chla)}(\lambda)$
385 coefficients determined for the three particle size classes have similar values, slight differences can be observed in the spectral range of 500 - 680 nm, where $a_p^{(Chla)}(\lambda)$ for the medium particle class has lower values than for the large classes and small particles. With the standard deviations determined for each mean taken into account, it is impossible to unambiguously separate the individual absorption spectra to determine which particle size class it may belong to. In the case of the average $a_p^{(SPM)}(\lambda)$ coefficients, there is a clear difference between the average determined for the micro particle class, which, together with the
390 standard deviations, varies from the average ± SD for the medium and small particle classes. The average $a_d^{(Chla)}(\lambda)$ and $a_d^{(SPM)}(\lambda)$ coefficients show slightly greater variation. The $a_d^{(Chla)}(\lambda)$ means clearly distinguish size classes, but if we take into

account the standard deviations, the possibility of qualifying the spectrum to a given size class of particles decreases. As in the case of $a_p^{(SPM)}(\lambda)$, the coefficients $a_d^{(SPM)}(\lambda)$ clearly distinguish the class of large particles from other particles. The average $a_{ph}^{(Chl a)}(\lambda)$ coefficients together with the standard deviations also do not allow separating the particle size classes clearly from

395 each other, however, there is a clear difference between the mean determined for large particles and the average for medium and small particles. On the other hand, the average coefficients $a_{ph}^{(SPM)}(\lambda) \pm$ SD make it possible to clearly distinguish the class of micro particles from the rest of the particles with sizes up to 20 μm.

The same analyzes were carried out for four distinguished particle size classes: micro (20-200 μm), nano (5-20 μm), ultra (2-5 μm) and pico (< 2 μm) and the results are summarized in Figure 10. For each particle size class analysis, it was

400 possible to determine the average chlorophyll-specific coefficients $a_p^{(Chl a)}(\lambda)$, $a_d^{(Chl a)}(\lambda)$ and $a_{ph}^{(Chl a)}(\lambda)$, and the average mass-specific coefficients $a_p^{(SPM)}(\lambda)$, $a_d^{(SPM)}(\lambda)$ and $a_{ph}^{(SPM)}(\lambda)$ with standard deviations (left and right panels, respectively, Figure 10). For the analyzed dataset, it is not possible to unambiguously separate the absorption coefficients into size classes. Only in the case of coefficients $a_d^{(Chl a)}(\lambda)$ it is possible to distinguish the class of micro-particles from ultra-particles in the spectral range above approx. 550nm.

405 Regardless of the division into 3 or 4 size classes, the obtained average spectra for the dominant size class do not clearly explain the shape of the absorption spectrum. According to Ciotti et al. (2002), average chlorophyll-specific light absorption coefficients have the lowest values for microplankton, then nanoplankton, and ultraplankton, and the highest values for the specific light absorption coefficient for picoplankton. These average spectra were determined by size fractionating for the coastal waters of Oregon, the shelf waters of the Bering Sea, and the Bedford Basin (Nova Scotia, Canada). Such an

410 arrangement of average specific absorption coefficients is related to the packing effect of pigments, where in larger particles there may be shading, and therefore less light absorption. In this work, for the Baltic data, the average chlorophyll-specific absorption coefficients are the lowest for nano-, then ultra- and picoplankton, and the highest for microplankton. Average values of $a_{ph}^{(Chl a)}(443)$ for micro, nano, ultra and pico-size classes by Ciotti et al. (2002) were approximately 0.012 m^2 mg^{-1}, 0.03 m^2 mg^{-1}, 0.042 m^2 mg^{-1} and 0.068 m^2 mg^{-1}, respectively. For the data analyzed in this article, the values of $a_{ph}^{(Chl a)}(443)$

415 for the micro, nano, ultra and pico-size classes are characterized by higher values, respectively 0.122 m^2 mg^{-1}, 0.057 m^2 mg^{-1}, 0.082 m^2 mg^{-1} and 0.112 m^2 mg^{-1}.

The average determined for the micro-size class is probably overestimated and this applies to all absorption coefficients a_p, a_d, and a_{ph}. This is due to the fact that the Chl$a$_fraction/Chl$a$ or SPM_fraction/SPM predominance condition was met only in 2 cases, the absorption spectra of which differed significantly from each other. Both cases relate to samples

420 collected at the pier in Sopot, one at the end of March (SF04 - Secchi disk was 5.5 m, the bottom was 6 m) and the other at the end of August (SF13 - Secchi disk was 1.5 m, the bottom was at 6 m, there was a large wave, so there was probably mixing with the bottom particles as well). For the SF04 sample, the concentrations of Chl$a$ and SPM were 0.78 mg m^{-3} and 1.99 g m^{-3}, respectively, for the original samples, and the light absorption coefficients of the particles were low. For the micro size class Chl$a$ and SPM were 0.41 mg m^{-3} and 0.92 g m^{-3}, respectively. However, for the SF13 sample, Chl$a$ and SPM were 4.05 mg

425 m^{-3} and 15.24 g m^{-3}, respectively, for the original samples, and the light absorption coefficients of the particles were an order

of magnitude higher than for SF04. For the micro size class, the Chl*a* and SPM concentrations were 1.87 mg m^{-3} and 8.97 g m^{-3}, respectively.
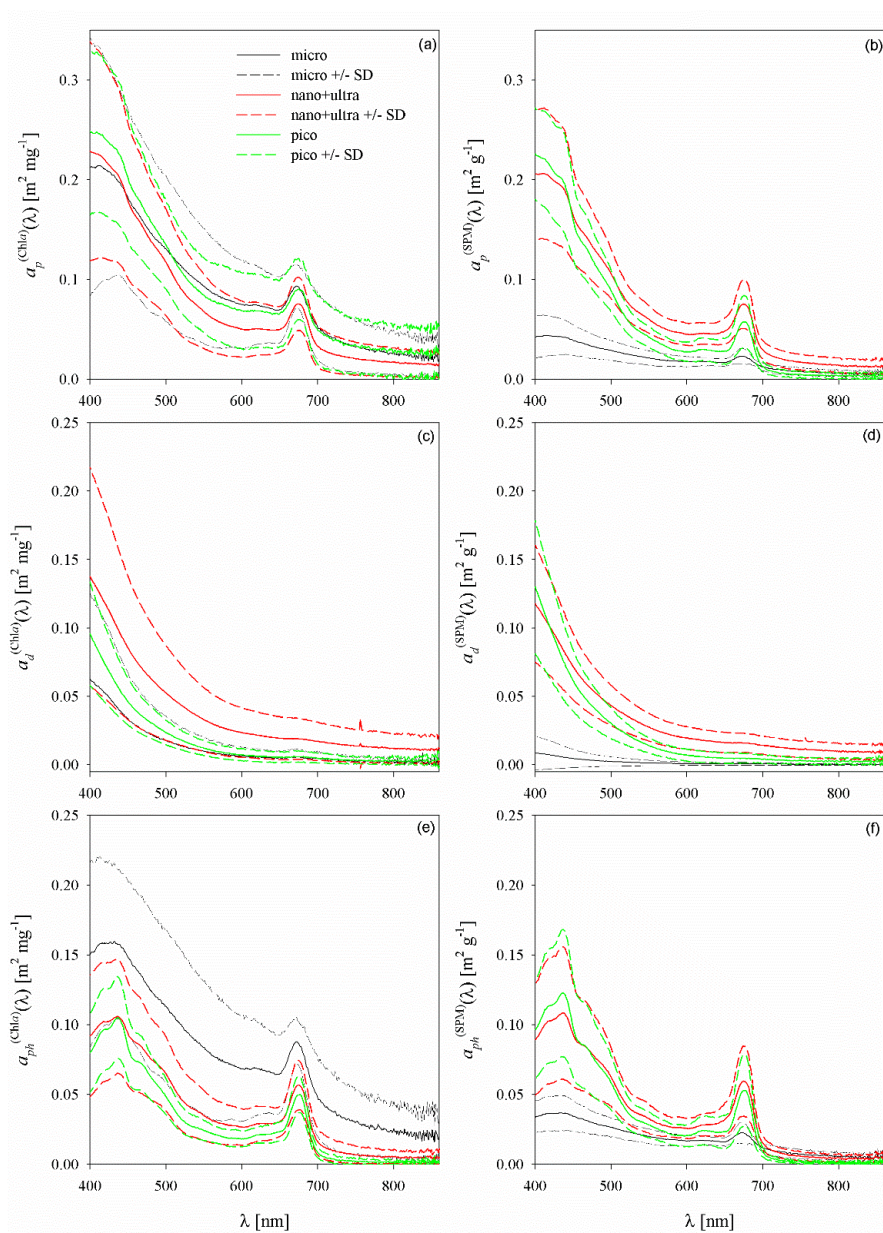
Figure 9: Mean chlorophyll-specific (left panel) and mass-specific (right panel) light absorption coefficients for all particles (a, b), detritus (c, d) and phytoplankton (e, f) for 3 size classes: micro-, nano-+ultra- and picoplankton. SD means standard deviation.
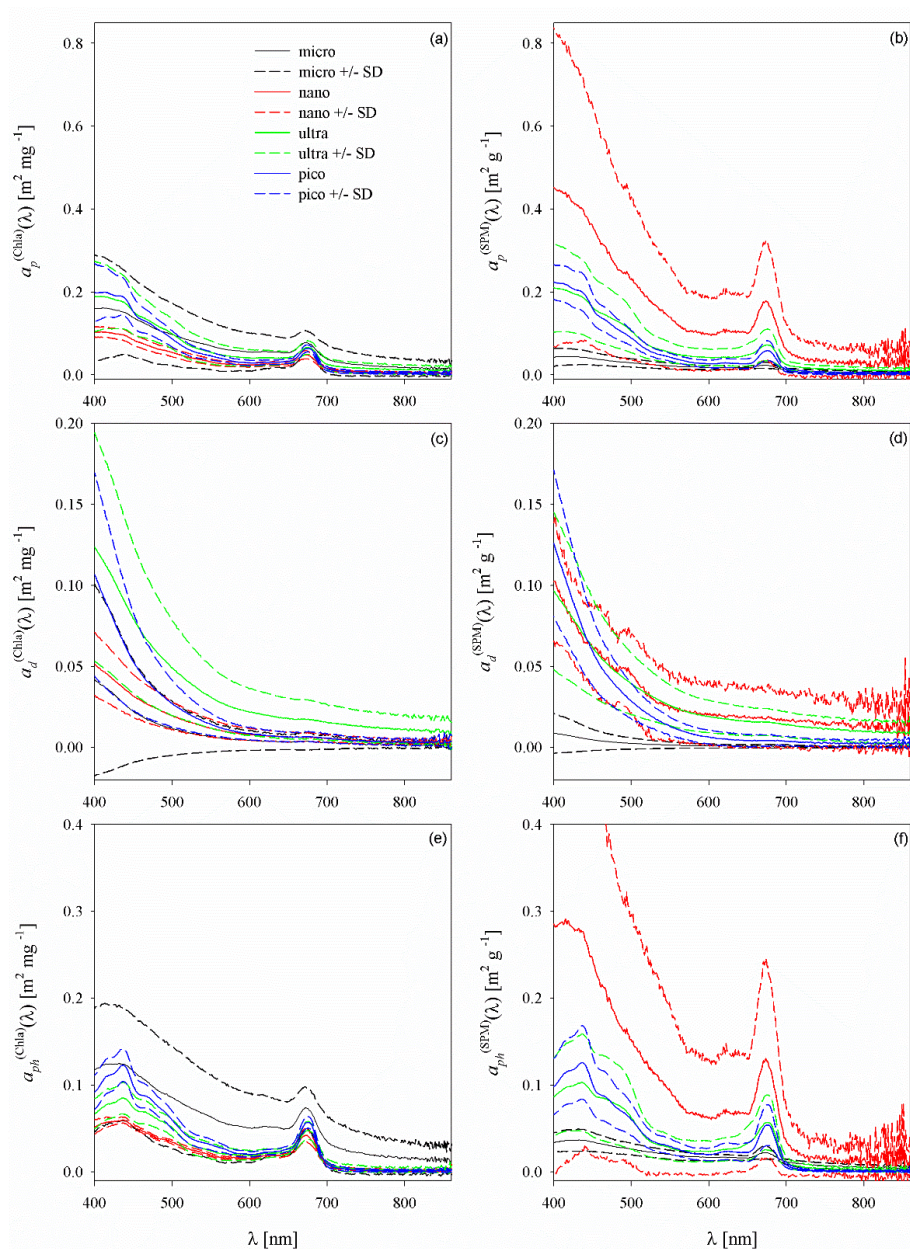
Figure 10: Mean chlorophyll-specific (left panel) and mass-specific (right panel) light absorption coefficients for all particles (a, b), detritus (c, d) and phytoplankton (e, f) for 4 size classes: micro-, nano-, ultra- and picoplankton. SD means standard deviation.

435

As mentioned above, Mohammadpour et al. (2017) studied the optical properties of the SPM size fractions in the littoral waters of Quebec for the size classes 0.2–0.4 μm, 0.4–0.7 μm, 0.7-10 μm and >10 μm. Among other things, mass-specific coefficients of light absorption by various size fractions of suspensions for different regions of the studied water body

were presented. Due to the difference in the determination of size fractions, we can only conclude that the tested waters within
440   Quebec are dominated by mineral suspensions, while the particles from the Baltic Sea waters analyzed in this work are
dominated by organic suspensions. Mohammadpour et al. (2017) report spatial differentiation of the contribution of different
size fractions of the suspension, which results in a large differentiation of light absorption coefficients. For the 0.2-0.7 μm size
classes, this variability ranges from close to zero to > 0.4 mg^2 g^{-1} at 400 nm wavelength. Similar differentiation was observed
for the fraction >10 μm. Mohammadpour et al. (2017) did not report averaged specific mass factors $a_p^{(SPM)}(\lambda)$. However, their
445   variability is similar to that presented in the Baltic Sea dataset, except that our spectra are characterized by clear chlorophyll
maxima in the green (400-460 nm) and red (660-690 nm) bands.

4 Conclusions

Our research presented in this paper provided important information on the role of particle size and composition in
light absorption by size fractions of suspensions in the waters of the Baltic Sea. Particles of different size classes may show
450   large variability in the absorption properties, with the ranges of variability for small and large particles overlapping. This can
cause difficulties in identifying the particle size class on the basis of the light absorption spectrum.

In this work, for the first time in the history of research on the optical properties of the Baltic Sea waters, we have
quantitatively shown different budgets/proportions of light absorption by particles of different size classes based on the analysis
of 38 sets of data from both open waters and coastal areas of the Baltic Sea. Despite the complicated relationship between the
455   influence of particle size and composition on light absorption, we observed that particles with sizes < 5 μm often had a major
contribution to $a_p(443)$, $a_d(443)$ and $a_{ph}(443)$, which was more than 60 %. The particle sizes from 5 μm to 20 μm had
contribution of $a_p(443)$, $a_d(443)$ and $a_{ph}(443)$ > 19 %, 27 % and 18 %, respectively. On the other hand, particles > 20 μm had
contributions in $a_p(443)$, $a_d(443)$ and $a_{ph}(443)$ > 6 %, 4 % and 8 %, respectively.

Measurements of mass-specific and chlorophyll-specific light absorption coefficients of suspended particles,
460   including detritus and phytoplankton, are essential for developing optical inversions to mapping biogeochemical components
found in surface waters and to better understand the origin of optical signatures in remote sensing studies. We determined the
relationships a_p, a_d, a_{ph} vs Chl*a* and SPM for the wavelength of 443 nm. This type of relationship may be useful in local and
regional studies of the biogeooptical properties of suspensions. The relationships analyzed in this paper could be used to
create/improve a model of light absorption by suspension particles of various sizes in the Baltic Sea. In order to propose such
465   a model, further research is needed, supported in addition by the analysis of particle size distributions (PSD).

So far, the literature has not presented comprehensive analyzes of the variability of light absorption coefficients by
different size fractions of particles suspended in seawater. Most studies on fractionation by particle size, mainly phytoplankton,
have been carried out by determining Chl*a* concentrations and then the value of primary production (Decembrini et al., 2014;
Deng et al., 2022; Hamasaki et al., 1998; Kormas et al., 2002; Maranon et al., 2001; Cermeno et al., 2005). On the contrary,
470   for all studies of suspended marine solids, size fractionation was carried out mainly to determine the chemical composition of
suspended solids (Lam et al., 2017, 2018; Xiang and Lam, 2020; Yigiterhan et al. 2020). In turn, Koestner et al. (2019)

investigated the effect of particle size and composition on light scattering in fractionated seawater samples for coastal and estuarine waters in the region of San Diego, California. The relationships of a_p, a_d, a_{ph} coefficients on Chl$a$ or SPM were shown only for the total suspension, not taking into account the size. However, the relationships presented by other authors were obtained indirectly, but on the basis of, for example, the analysis of diagnostic pigments (DPA) and the size structure (Vidussi et al., 2001; Uitz et al., 2008) or on the basis of HPLC data and the pigment size-class model (Brewin et al. 2010). Brewin et al. (2011) extended the two-factor model of Sathyendranath et al. (2001) and Devred et al. (2006) to a three-component model of light absorption by size fractions. A similar task was undertaken by Hirata et al. (2008) and Aiken et al. (2009). Only studies by Ciotti et al. (2002) showed the actual variability (not modeled) of light absorption coefficients by phytoplankton in size classes for waters of the Bering Sea and coastal waters of Oregon. While Mohammadpour et al. (2017) presented the variability of the light absorption coefficients of all suspended particles in size classes (0.2-0.4 μm, 0.4-0.7 μm, 0.7-10 μm, > 10 μm) in estuarine waters of the Saint Lawrence River and a major SLE tributary, the Saguenay Fjord.

This work is unique not only when it comes to studying the optical properties of the Baltic Sea waters, but also stands out in the international arena of research on the absorption of light by particles in various size fractions. Its main advantage is that it is based on real (not modelled) data.

Data availability:

The *in situ* light absorption data (absorption by particles, detritus, phytoplankton and CDOM) and biogeochemical data (concentration of Chl$a$ and SPM) can be acquired for scientific research purposes upon request from Justyna Meler

Authors contribution:

Conceptualization, J.M.; methodology, J.M. and M.Z.; validation, J.M, M.Z. and D.L.; formal analysis, J.M.; investigation, J.M.; resources, J.M, D.L., M.Z., data curation, J.M., M.Z.; writing—original draft preparation, J.M.; writing—review and editing, M.Z. and D.L.; visualization, J.M.; supervision, M.Z., All authors have read and agreed to the published version of the manuscript.

Conflicts of Interest:

The authors declare that they have no conflict of interest.

Acknowledgments:

This research was carried out as part of the project funded by the National Science Centre, Poland, entitled 'Investigating the variability of the spectra of light absorption coefficients by various size fractions of suspended matter occurring in the southern area of the Baltic Sea' (contract No. 2020/04/X/ST10/00335) (awarded to Justyna Meler). We are grateful to the Institute of Oceanology Polish Academy of Sciences in Sopot, represented by Sławomir B. Woźniak, Joanna Stoń-Egiert and Karolina Borzycka for their help in collecting the empirical material.

References

Aiken, J., Pradhan, Y., Barlow, R., Lavender, S., Poulton, A., Holligan, P., and Hardman-Mountford, N.: Phytoplankton pigments and functional types in the Atlantic Ocean: A decadal assessment, 1995–2005, Deep Sea Res. Part II: Topical Studies
505 in Oceanography, Vol. 56(15), 2009, 899-917, https://doi.org/10.1016/j.dsr2.2008.09.017, 2009.

Babin, M., Stramski, D., Ferrari, G.M., Claustre, H., Bricaud, A., Obolensky, G., and Hoepffner, N.: Variations in the light absorption coefficient of phytoplankton, nonalgal particles, and dissolved organic matter in coastal waters around Europe. J. Geophys. Res., 108(C8):3211, https://doi.org/10.1029/2001JC000882, 2003.

Bidigare, R.R., Morrow, J.H., and Kiefer, D.A.: Derivative analysis of spectral absorption by photosynthetic pigments in the
510 western Sargasso Sea, J. Mar. Res., 47, 323-341, 1989.

Brewin, R.J.W., Devred, E., Sathyendranath, S., Lavender, S.J., and Hardman-Mountford, N.J.: Model of phytoplankton absorption based on three size classes. Applied Optics, 50(22), 4535–4549. https://doi.org/10.1364/AO.50.004535, 2011.

Brewin R.J.W., Sathyendranath S., Hirata T., Lavender S.J., Barciela R.M., and Hardman-Mountford N.J.: A three-component model of phytoplankton size class for the Atlantic Ocean, Ecol. Model. 221, 1472–1483,
515 https://doi.org/10.1016/j.ecolmodel.2010.02.014, 2010.

Brewin R.J.W., Hirata T., Hardman-Mountford N.J., Lavender S.J., Sathyendranath S., and Barlow R.: The influence of the Indian Ocean Dipole on interannual variations in phytoplankton size structure as revealed by Earth Observation, Deep-Sea Res. II, 77-80, 117-127, https://doi.org/10.1016/j.dsr2.2012.04.009, 2012.

Bricaud, A., and Stramski, D.: Spectral absorption coefficients of living phytoplankton and nonalgal biogenous matter: A
520 comparison between the Peru upwelling area and the Sargasso Sea. Limnology and Oceanography, 35(3), 562–582. https://doi.org/10.4319/lo.1990.35.3.0562, 1990.

Bricaud, A., Claustre, H., Ras, J., and Oubelkheir, K.: Natural variability of phytoplankton absorption in oceanic waters: influence of the size structure of algal populations, J. Geophys. Res., 109, C11010, https://doi.org/10.1029/2004JC002419, 2004.

525 Bricaud, A., Ciotti, A.M, and Gentili, B.: Spatial-temporal variations in phytoplankton size and colored detrital matter absorption at global and regional scales, as derived from twelve years of SeaWiFS data (1998–2009), Global Biogeochemical Cycles, 26(1), https://doi.org/10.1029/2010GB003952, 2012.

Castagna, A., Amadei Martínez, L., Bogorad, M., Daveloose, I., Dasseville, R., Dierssen, H. M., Beck, M., Mortelmans, J., Lavigne, H., Dogliotti, A., Doxaran, D., Ruddick, K., Vyverman, W., and Sabbe, K.: Optical and biogeochemical properties
530 of diverse Belgian inland and coastal waters, Earth Syst. Sci. Data, 14, 2697–2719, https://doi.org/10.5194/essd-14-2697-2022, 2022.

Cermeño, P., Estévez-Blanco, P., Marañón, E., and Fernóndez, E.: Maximum photosynthetic efficiency of size-fractionated phytoplankton assessed by 14C uptake and fast repetition rate fluorometry, Limnol. and Oceanogr., 5, https://doi.org/10.4319/lo.2005.50.5.1438, 2005.

535 Ciotti, A.M., and Bricaud, A.: Retrievals of a size parameter for phytoplankton and spectral light absorption by colored detrital matter from water-leaving radiances at SeaWiFS channels in a continental shelf region off Brazil. Limnology and Oceanography Methods, 4, 237–253. https://doi.org/10.4319/lom.2006.4.237, 2006.

Ciotti, A.M., Lewis, M.R., and Cullen, J.J.: Assessment of the relationships between dominant cell size in natural phytoplankton communities and the spectral shape of the absorption coefficient, Limnol. Oceanogr. 47(2), 404–417, 2002.

540 Davies, E.J., McKee, D., Bowers, D., Graham, G.W., and Nimmo-Smith, W.A.M.: Optically significant particle sizes in seawater. Appl. Opt. 53: 1067–1074, https://doi.org/10.1364/AO.53.001067, 2014.

Decembrini, F., Bergamasco, A., and Mangoni, O.: Seasonal characteristics of size-fractionated phytoplankton community and fate of photosynthesized carbon in a sub-Antarctic area (Straits of Magellan), J. Mar. Sys., 136, 31-41, http://dx.doi.org/10.1016/j.jmarsys.2014.03.008, 2014.

545 Deng, L., Zhou, W., Xu, J., Cao, W., Liao, J., and Zhao, J.: Estimation of vertical size-fractionated phytoplankton primary production in the northern South China Sea, Ecological Indicators, 135, 103546, https://doi.org/10.1016/j.ecolind.2022.108546, 2022.

Devred E., Sathyendranath S., Stuart V., and Platt T.: A three component classification of phytoplankton absorption spectra: Application to ocean-color data, Remote Sens. Environ.115, 2255-2266, https://doi.org/10.1016/j.rse.2011.04.025, 2011.

550 Devred, E., Sathyendranath, S., Stuart, V., Maas, H., Ulloa, O., and Platt, T.: A two-component model of phytoplankton absorption in the open ocean: Theory and applications. J. Geophys. Res., 111: C03011, https://doi.org/10.1029/2005JC002880, 2006.

D'Sa, E.J., and Ko, D.S.: Short-term influences on suspended particulate matter distribution in the Northern Gulf of Mexico: Satellite and model observations, Sensors, 8, 4249–4264, https://doi.org/10.3390/s8074249, 2008.

555 D'Sa, E.J., Miller, R.L., and Del Castillo, C.: Bio-optical properties and ocean color algorithms for coastal waters influenced by the Mississippi River during a cold front, Appl. Optics, 45, 7410–7428, https://doi.org/10.1364/AO.45.007410, 2006.

Eleveld, M.A., van der Wal, D., and van Kessel, T.: Estuarine suspended particulate matter concentrations from sunsynchronous satellite remote sensing: Tidal and meteorological effects and biases, Remote Sens. Environ., 143, 2014–215, https://doi.org/10.1016/j.rse.2013.12.019, 2014.

560 Ferreira, A., Stramski, D., Garcia, C.A.E., Garcia, V.M.T., Ciotti, A.M., and Mendes, C.R B.: Variability in light absorption and scattering of phytoplankton in Patagonian waters: Role of community size structure and pigment composition, J. Geophys. Res. Oceans, 118, 698–714, https://doi.org/10.1002/jgrc.20082, 2013.

Hamasaki, K., Ikeda, M., Ishikawa, M., Shirasawa, K., and Taguchi, S.: Seasonal variability of size-fractionated chlorophyll a in Monbetsu Harbor, Hokkaido, northern Japan, Plankton Biol. Ecol., 45(2), 151-158, 1998.

565 Hirata T., Aiken J., Hardman-Mountford N.J., Smyth T.614 J., and Barlow R.G.: An absorption model to determine phytoplankton size classes from satellite ocean colour , Remote Sens. Environ.112, 3153–3159, https://doi.org/10.1016/j.rse.2008.03.011, 2008.

Hirata T., Hardman-Mountford N.J., Brewin R.J.W., Aiken J., Barlow R.G., Suzuki K., Isada T., Howell E., Hashioka T., Noguchi-Aita M., and Yamanaka Y.: Synoptic relationships between surface Chlorophyll-a and diagnostic pigments specific

570   to phytoplankton functional types, Biogeosciences, 8, 311-327, https://doi.org/10.5194/bg-8-311-2011, 2011.

Hoepffner, N., and Sathyendranath, S.: Bio-optical characteristics of coastal waters: Absorption spectra of phytoplankton and pigment distribution in the western North Atlantic, 37(8), 1160-1179, https://doi.org/10.4319/lo.1992.37.8.1660, 1992.

IOCCG (2014), Phytoplankton functional types from space, Sathyendranath, S. (ed.), Reports of the International Ocean-Colour Coordinating Group, No. 15, IOCCG, Dartmouth, Canada,154 pp., 2014.

575   Kheireddine M., Ouhssain M., Organelli E., Bricaud A., and Jones B.H.: Light absorption by suspended particles in the Red Sea: effect of phytoplankton community size structure and pigment composition, J. Geophys. Res.-Oceans, 123, 1-20, https://doi.org/10.1002/2017JC013279, 2018.

Koestner, D., Stramski, D., and Reynolds, R.: Assessing the effects of particle size and composition on light scattering through measurements of size-fractioned seawater samples, Limnol. Oceanogr., 9999, 1-18, https://doi.org/10.1002/lno.11259, 2019.

580   Kormas, K.A., Garametsi, V., and Nicolaidou, A.: Size-fractioned phytoplankton chlorophyll in an Eastern Mediterranean coastal system (Maliakos Gulf, Greece), Helgol Mar. Res., 56, 125-133, https://doi.org/10.1007/s10152-002-0106-2, 2002.

Kowalczuk, P., Stedmon, C.A., and Markager, S.: Modeling absorption by CDOM in the Baltic Sea from season, salinity and chlorophyll, Mar. Chem. 101(1–2), 1–11, https://doi.org/10.1016/j.marchem.2005.12.005, 2006.

Kowalczuk, P., Sagan, S., Zabłocka, and, M., Borzycka, K.: Mixing anomaly in deoxygenated Baltic Sea deeps indicates

585   benthic flux and microbial transformation of chromophoric and fluorescent dissolved organic matter, Estuar. Coast. Shelf S. 163, PB, 206-217, https://doi.org/10.1016/j.ecss.2015.06.027, 2015.

Lam, P.J., Ohnemus, D.C.,and Auro, M.E.: Size-fractioned major particle composition and concentrations from the US GEOTRACES North Atlantic Zonal Transect. Deep Sea Research Part II: Topical Studies in Oceanography, 116, 303– 320, https://doi.org/10.1016/j.dsr2.2014.11.020, 2015.

590   Lam, P.J., Lee, J.-M., Heller, M.I., Mehic, S., Xiang, Y., and Bates, N.R.: Size-fractioned distributions of suspended particle concentration and major phase composition from the U.S. GEOTRACES Eastern Pacific Zonal Transect (GP16), Mar. Chem., 201, 90-107, http://dx.doi.org/10.1016/j.marchem.2017.08.013, 2018.

Le Quéré, C., Harrison, S.P., Prentice, C.I., Buitenhuis, E.T., Aumont, O., Bopp, L., Claustre, H., Cotrim da Cunha, L., Geider, R., Giraud, X., Klass, C., Kohfeld, K.E., Legendre, L., Manizza, M., Platt, T., Rivkin, R., Sathyendranath, R.B., Uitz, J.,

595   Watson, A.J., and Wolf-Gladrow, D.: Ecosystem dynamics based on plankton functional types for global ocean biogeochemistry models. Global Change Biol. 11(11): 2016–2040, https://doi.org/10.1111/j.1365-2486.2005.1004.x, 2005.

Loisel, H., and Stramski, D.: Estimation of the inherent optical properties of natural waters from the irradiance attenuation coefficient and reflectance in the presence of Raman scattering. Appl. Optics 30(18): 3001–3011, https://doi.org/10.1364/AO.39.003001, 2000.

600 Loisel, H., and Poteau, A.: Inversion of IOP based on Rrs and remotely retrieved Kd. In: Remote Sensing of Inherent Optical
Properties: Fundamentals, Tests of Algorithms, and Applications, Lee, Z.P. (Ed.), Reports of the International Ocean Colour
Coordinating Group, No. 5. IOCCG, Dartmouth, Canada, pp. 35–41, 2006.

Lorenzen, C.J.: Determination of chlorophyll and pheo-pigments: spectrophotometric equations, Limnol. Oceanogr., 12,
https://doi.org/10.4319/lo.1967.12.2.0343, 1967.

605 Marañón, E., Holligan, P.M., Barciela, R., González, N., Mouriño, B., Pazó, M.J., and Varela, M.: Patterns of phytoplankton
size structure and productivity in contrasting open-ocean environments, Mar. Ecol. Prog. Ser., 216, 43-56,
https://www.jstor.org/stable/24864737, 2001.

Marker, A.F., Nush, E.A., Rai, H., and Riemann, B.: The Measurement of Photosynthetic Pigments in Freshwaters and
Standardization of Methods: Conclusions and Recommendations. Archives fur Hydrobiologie, 14, 91-106, 1980.

610 McKee, D., and Cunningham, A.: Identification and characterisation of two optical water types in the Irish Sea from in situ
inherent optical properties and seawater constituents, Est. Coast. Shelf Sci., 68(1-2), 305-316,
https://doi.org/10.1016/j.ecss.2006.02.010., 2006.

Meler, J., Ostrowska, M., and Stoń-Egiert, J.: Seasonal and spatial variability of phytoplankton and non-algal absorption in the
surface layer of the Baltic. Estuar. Coast. Shelf S. 180:123-135, https://doi.org/10.1016/j.ecss.2016.06.012, 2016b.

615 Meler, J., Kowalczuk, P., Ostrowska, M., Ficek, D., Zabłocka, M., and Zdun, A.: Parameterization of the light absorption
properties of chromophoric dissolved organic matter in the Baltic Sea and Pomeranian Lakes. Ocean Sci. 12, 1013-1032,
https://doi.org/10.5194/os-12-1013-2016, 2016a.

Meler, J., Stoń-Egiert, J., and Woźniak, S.B.: Parameterization of phytoplankton spectral absorption coefficients in the Baltic
Sea: general, monthly and two-component variants of approximation formulas. Ocean Sci. 14, 1523–1545,
620 https://doi.org/10.5194/os-14-1523-2018, 2018.

Meler, J., Woźniak, S.B., and Stoń-Egiert, J.: Comparison of methods for indirectly estimating the phytoplankton population
size structure and their preliminary modifications adapted to the specific conditions of the Baltic Sea, J. Mar. Sys, 212, 103446,
https://doi.org/10.1016/j.jmarsys.2020.103446, 2020.

Meler, J., Ostrowska, M., Stoń-Egiert, J., and Zabłocka, M.: Seasonal and spatial variability of light absorption by suspended
625 particles in the southern Baltic: a mathematical description, J. Mar. Sys., 170, 68–87,
https://doi.org/10.1016/j.jmarsys.2016.10.011, 2017.

Mohammadpour, G., Gagné, J.-P., Larouche, P., and Montes-Hugo, M.A.: Optical properties of size fractions of suspended
particulate matter in littoral waters of Québec, Biogeosciences, 14, 5297-5312, https://doi.org/10.5194/bg-14-5297-2017,
2017.

630 Moisan, J.R., Moisan, T.A.H., and Linkswiler, M.A.: An inverse modeling approach to estimating phytoplankton pigment
concentrations from phytoplankton absorption spectra, J. Geophys. Res., 116, C09018, https://doi.org/10.1029/2010JC006786,
2011.

Morel, A., and Bricaud., A.: Theoretical results concerning light absorption in a discrete medium, and application to specific absorption of phytoplankton. Deep-Sea Res. 28(11):1375–1393, https://doi.org/10.1016/0198-0149(81)90039-X, 1981.

635 Mouw, C.B., and Yoder, J.: Optical determination of phytoplankton size composition from global SeaWiFS imagery. J. Geophys. Res. 115: C12018, https://doi.org/10.1029/2010JC006337, 2010.

Mouw, C.B., Hardman-Mountford, N.J., Alvain, S., Bracher, A., Brewin, R.J.W., Bricaud, A., Ciotti, A., Devred, E., Fujiwara, A., Hirata, T., Hiraweke, T., Kostadinov, T.S., Roy, S., and Uitz., J.: A consumer's guide to satellite remote sensing of multiple phytoplankton groups in the global ocean. Ocean. Front. Mar. Sci.4:41, https://doi.org/10.3389/fmars.2017.00041, 2017.

640 Organelli, E., Bricaud, A., Antoine, D., and Uitz, J.: Multivariate approach for the retrieval of phytoplankton size structure from measured light absorption spectra in the Mediterranean Sea (BOUSSOLE site). Applied Optics, 52(11), 2257–2273. https://doi.org/10.1364/AO.52.002257, 2013.

Pearlman, S.R., Costa, H.S., Jung, R.A., McKeown, J.J., and Pearson, H.E.: Solids (section 2540). In: Eaton, A.D., Clesceri, L.S., Greenberg, A.E. (Eds.), Standard Methods for the Examination of Water and Wastewater. American Public Health
645 Association, Washington, D.C., 2–53–2–64, 1995.

Platt, T., and Sathyendranath, S.: Ecological indicators for the pelagic zone of the ocean from remote sensing. Remote Sensing of Environment, 112: 3426-3436, https://doi.org/10.1016/j.rse.2007.10.016, 2008.

Saggiomo, V., Goffart, G., Carrada, G.C., and Hecq, J.H.: Spatial patterns of phytoplanktonic pigments and primary production in a semi-enclosed periantarctic ecosystem: the Strait of Magellan, J. Mar. Sys., 5(2), 119-142, https://doi.org/10.1016/0924-
650 7963(94)90027-2, 1994.

Sathyendranath, S., Lazzara, L., and Prieur, L.: Variations in the spectral values of specific absorption of phytoplankton, Limnology and Oceanography, 32, doi: 10.4319/lo.1987.32.2.0403, https://doi.org/10.4319/lo.1987.32.2.0403, 1987.

Sathyendranath S., Cota, G., Stuart, V., Maass, H., and Platt, T.: Remote sensing of phytoplankton pigments: a comparison of empirical and theoretical approaches. Int. J. Remote Sens. 22: 249–273, https://doi.org/10.1080/014311601449925, 2001.

655 Sieburth, J.M., Smetacek, V., and Lenz, J.: Pelagic ecosystem structure: heterotrophic compartments of the plankton and their relationship to plankton size fractions. Limnol. Oceanogr. 23, 1256–1263, https://doi.org/10.4319/lo.1978.23.6.1256, 1978.

Stedmon, C.A., Markager, S., and Kaas, H.: Optical properties and signatures of chromophoric dissolved organic matter (CDOM) in Danish coastal waters. Estuarine, Coastal and Shelf Science 51, 267–278, https://doi.org/10.1006/ecss.2000.0645, 2000.

660 Stramski, D., Reynolds R.I., Kaczmarek, S., Uitz, J., and Zheng, G.: Correction of pathlength amplification in the filter-pad technique for measurements of particulate absorption coefficient in the visible spectral region. Applied Optics 54(22):6763-6782, https://doi.org/10.1364/AO.54.006763, 2015.

Strickland, J.D.H., and Parsons, T.R.: A practical handbook of seawater analyses. Fisheries Research Board of Canada. Ottawa, https://doi.org/10.1002/iroh.19700550118, 1972.

665 Uitz J., Claustre H., Morel A., and Hooker S.B.: Vertical distribution of phytoplankton communities in open ocean: An assessment based on surface chlorophyll, J. Geophys. Res. 111, C08005, https://doi.org/10.1029/2005JC003207, 2006.

Uitz, J., Huot, Y., Bruyant, F., Babin, M., and Claustre, H.: Relating phytoplankton photophysiological properties to community structure on large scales. Limnol. Oceanogr. 53(2): 614–630, https://doi.org/10.4319/lo.2008.53.2.0614, 2008.

Vidussi, F., Claustre, H., Manca, B.B., Luchetta, A., and Marty, J.C.: Phytoplankton pigment distribution in relation to upper
670 thermocline circulation in the eastern Mediterranean Sea during winter. Journal of Geophysical Research, 106(C9), 19939–19956. https://doi.org/10.1029/1999JC000308, 2001.

Wintermans, J.F.G.M., and De Mots, A.: Spectrophotometric characteristics of chlorophylls a and b and their phenophytins in ethanol, Biochimica et Biophysica Acta (BBA) - Biophysics including Photosynthesis, Volume 109, Issue 2, 448-453, https://doi.org/10.1016/0926-6585(65)90170-6, 1965.

675 Woźniak, S.B., and Meler, J.: Modelling Water Colour Characteristics in an Optically Complex Nearshore Environment in the Baltic Sea; Quantitative Interpretation of the Forel-Ule Scale and Algorithms for the Remote Estimation of Seawater Composition. Remote Sens., 12, 2852, https://doi.org/10.3390/rs12172852, 2020.

Woźniak, S.B., Meler, J., Lednicka, B., Zdun, A., and Stoń-Egiert, J.: Inherent optical properties of suspended particulate matter in the southern Baltic Sea. Oceanologia. 53(3):691-729, https://doi.org/10.5697/oc.53-3.691, 2011.

680 Woźniak, S.B., Sagan, S., Zabłocka, M., Stoń-Egiert, J., and Borzycka, K.: Light scattering and backscattering by particles suspended in the Baltic Sea in relation to the mass concentration of particles and the proportions of their organic and inorganic fractions. J. Mar. Syst. 182, 79–96. https://doi.org/10.1016/j.jmarsys.2017.12.005, 2018.

Woźniak, S.B., Meler, J., and Stoń-Egiert, J.: Inherent optical properties of suspended particulate matter in the southern Baltic Sea in relation to the concentration, composition and characteristics of the particle size distribution; new forms of
685 multicomponent parameterizations of optical properties. Journal of Marine Systems, 229, 10372, https://doi.org/10.1016/j.jmarsys.2022.103720, 2022.

Xiang, Y., and Lam, P.J.: Size-fractionated compositions of marine suspended particles in the western Arctic Ocean: Lateral and vertical sources. J. Geoph. Res.: Oceans, 125, e2020JC016144. https://doi.org/10.1029/2020JC016144, 2020.

Yigiterhan, O., Al-Ansari, E. M., Nelson, A., Abdel-Moati, M. A., Turner, J., Alsaadi, H. A., Paul, B., Al-Maslamani, I. A.,
690 Al-Ansi Al-Yafei, M. A., and Murray, J. W.: Trace element composition of size-fractionated suspended particulate matter samples from the Qatari Exclusive Economic Zone of the Arabian Gulf: the role of atmospheric dust, Biogeosciences, 17, 381–404, https://doi.org/10.5194/bg-17-381-2020, 2020.

Zhang, X., Huot, Y., Bricaud, A., and Sosik, H.: Inversion of spectral absorption coefficients to infer phytoplankton size classes, chlorophyll concentration, and detrital matter, Appl. Opt. 54, 5805-5816, https://doi.org/10.1364/AO.54.005805,
695 2015.